University of Stavanger

Faculty of Science and Technology

MASTER'S THESIS

Study program/ Specialization: Master in Petroleum technology. Drilling and well technologies.	Spring semester, 2015 Open access
Writer: Yahor Makayonak	…… (Writer's signature)
Faculty supervisor: Bernt S. Aadnøy External supervisor(s): V.P. Balitsky	
Thesis title: Analysis of drill-string based on case study of ultra-deep drilling on Kola Peninsula.	
Credits (ECTS): 30	
Key words: Drill-string, tension, force, torque, alloy, load, material, well, azimuth, inclination, measured depth, strength, optimization.	Pages: ……53…… + enclosure: …0…… Stavanger, 15.06.2015

Abstract

The topic of the following project is devoted to the theme of drilling of the ultra-deep wells and in particular to the optimization of the length of dual aluminum-steel drill string as a one of the concept which have been used for drilling of super deep well on Kolskyi peninsula.

The mentioned project is the most prominent and successful representative of conducted in formal Soviet Union countries (FSU) program of super-deep scientific drilling in 70^{th}-90^{th} years of the last century. The program of super-deep borehole construction was in many senses a unique long-term field experiment. Several new drilling technologies have been developed at this time. Among them aluminum drill-pipes, gear reduction turbo-drills, coring tools for hard rock drilling, drilling and coring without pulling the drill-pipes (DWPP) in crystalline rocks, vertical drilling technology and a number of other improvements.

Interest of scientists to the composition and structure of the deep zones of the crust is inexhaustible and is always on the agenda. But the possibility of getting the unique scientific and technological data is limited to the actual level of scientific and technical progress. Modern simulators and software products together with experience based engineering approach allows us to consider in more detail the calculation of loads on the drill string and take into account a number of relevant factors. A suchlike working mechanism was not available to engineers thirty years ago and the work was generally based on intuitive knowledge and experience of the scientists and engineering community.

Outcome of the conducted project on Kolskyi peninsula was outstanding not only as a result for geological and geophysical areas, but also as an outcome in commercial drilling engineering. It gave an impulse for the further drilling technology development and played the role in the oil and gas drilling technology upgrading. Important to notice, that aluminium high strength drill-pipes was developed at this time and found successful application in offshore riser-less drilling. Aluminium drill-strings become a source of increased interest in the last decade mainly because of the hidden potentials for extended reach and horizontal drilling applications and improved drill rig capacity.

The issue of drilling of ultra-deep wells will increase in the future also due to normal growing interest of engineering community to drill an unreachable depth and to gain new high technological results. The topic may be of interest also for the wide range of companies involved in the development of reservoirs with extended reach depth.

Contents

1 Introduction

In the modern world the value of mineral resources is continuously increasing. Requires more oil and gas and others types of autonomous sours of energy. Increases use of aluminum, titanium, molybdenum and other alloying metals, chrome and nickel. Following the search of new sources of minerals and hydrocarbon resources humans began to explore the bottom of the shelf of the seas and World Ocean. Continuously increased the depth of exploration and development on the continents.

In this connection study of deep crustal structure is becoming increasingly important. Unexplored depths of the earth fraught with not only the answer to the origin and evolution of the earth's crust but also to still unknown natural resources. The humanity a long time ago is cared by the idea of exploration of deep crustal structure, but it became available only for the last decades.

Ultra deep drilling can be designated as the drilling of wells or boreholes to the depths of 6,000 m or more in order mainly to study the earth's crust and upper mantle and also to locate deposits of useful minerals and metal's ores. The term "ultra-deep drilling" appeared in the literature from the 1950's.

In the 1970's international Geodynamic Project was conducted and ultra-deep drilling was closely associated with this project. The program was coordinated by Inter-union Commission on Geodynamics (ICG) established by the International Council of the Scientific Union (ICSU). The aim was to obtain direct data related to the material composition and physical properties of the lower layers of the lithosphere and to explain the origin, structure, evidence of motions and development of these layers. Great emphasis has been placed on the importance of exploiting the new opportunities that have abruptly opened up in solid earth geology. The results of a major effort at this time are certain profound implication for basic science and the broad range of practical problems related to the solid earth environment.

Ultra-deep drilling makes it possible to determine the age of the geochemical and geophysical characteristics of the rocks composing in lithosphere, to study gaseous and liquid emanations from deep within the earth, and to determine the geological nature of physical fields, limits, and layers, as well as the temperature conditions and thermal radiation of the earth's interior. From the hydrocarbon exploration prospects ultra-deep drilling is used to evaluate the potential oil- and gas-bearing capacities of deep sedimentary basins and to conduct prospecting and exploration work of oil and gas deposits. It has also been proposed for use in studying earthquakes stress formations [1].

By 1974, more than 400 ultra-deep wells had been totally drilled. Among them the following wells been drilled on land: Bertha Rogers No. 1 (9,583 m) and Bayden Unit (9,160 m; both in Oklahoma, USA), Shevchenko No. 1 (7,024 m; western Ukraine, USSR), and Aralsor (6,806 m; Caspian Lowland, USSR) [1].

It is worth noting that ultra-deep drilling activities as any others branches had been stimulated by the cold war reality at that time, which became a driver for intensification of research activities and technological improvement between to competitive sides of the world.

As example USA had been announcing and developing the Mohole Project contained proposals for ocean drilling in the seabed to depths of several kilometres. In the actual master thesis we will focus on the ambitious Soviet project implemented on Baltic shield of Kolskyi Peninsula (northern-western part of the USSR, Russia at the present) started in 1970 and continued for around 20 years. A plan was to drill an ultra-deep well on land to depths of 13000 m but the final goal hasn't been achieved (reached depth of 12,262 km) due to material and technological limitation at that time and a certain indirect reasons related to the investment cut and corresponding historical conversions in the Soviet Union in the early 90-th.

One of the core elements of any ultra-deep drilling project becomes investigation and optimisation of reliable drill string. In the following thesis we will review the specific of drilling ultra-deep and take a look at the main problems and limiting factors. Will be reviewed the issue

of well bore stability geological and thermal conditions of the Kola location. Later in resent work conducting the broad analysis of field data and correlating with the computed we will find the certain dependency. A huge part of the work devoted to the key component of the drilling issue namely design of light alloying drilling string for ultra deep drilling.

We will try to describe breathily a complex approach implemented by Russians engineers and to look at the difficulties, challenges and limitations which had been faced while drilling 12 km long well. Together with experienced reader will try to implement and optimise the combined double material aluminium-steel drill-string length for long vertical well based on condition on the mentioned well and material limitations and calculate the vertical tension stresses on the drill string of 12260 m long.

Finely introducing of modern projects of ultra-deep drilling we will convince the interested reader in the absolute possibility and consistency of ultra-deep and extended length drilling theory using improved conventional approach.

2 Description of ultra-deep well on Kola Peninsula and it location

2.1 Purposes of the project on Kola Peninsula

Kola ultra-deep well situated on the north-western part of Murmansk region (Pechenga district) close to the Norwegian border (Fig.1). Kola Peninsula occupied the north-eastern part of Baltic shield. Here on the area of more than 1 million thousand km^2 including parts of Norway, Sweden, Finland and Russia mainly developed the most ancient geological formations.

Fig. 1 Geographical location of Kola well.

By the early 70-s the preparatory work for drilling of Kola well (fig.2) were completed. From that moment began the second phase of the project namely drilling the ultra deep well, which got the code name SG-3 (СГ-3 in Russian). The following purposes and targets were identified:

- explore the deep structure of the Pechenga (name of the location on Kola peninsula) nickel-bearing complex;
- clarify the geological nature of seismic border interface in the continental crust and get the new data about subsurface thermal regime, aqueous solutions and gases;
- to get maximum information about material composition of the rocks and it physical condition and to open the border zone between granite and basalt layers of the earth's crust;
- improve existing and create new technique and technology for ultra-deep drilling and also methods for complex geophysical investigation of rocks at a great depths [2].

Planed at the beginning for the ambitious depth of 13 km the well on Kola Peninsula reached the depth of 10,7 km by early 1980-th. Extreme depth and related technological complexity and challenge has led to the fact that in a next 10 years of work was achieved some certain progress of 1,5 km extra drilling. By the year of 1990 the final depth stopped at the level of 12262 m and to this day is still remaining the record of the deepest vertical well ever drilled in the world.

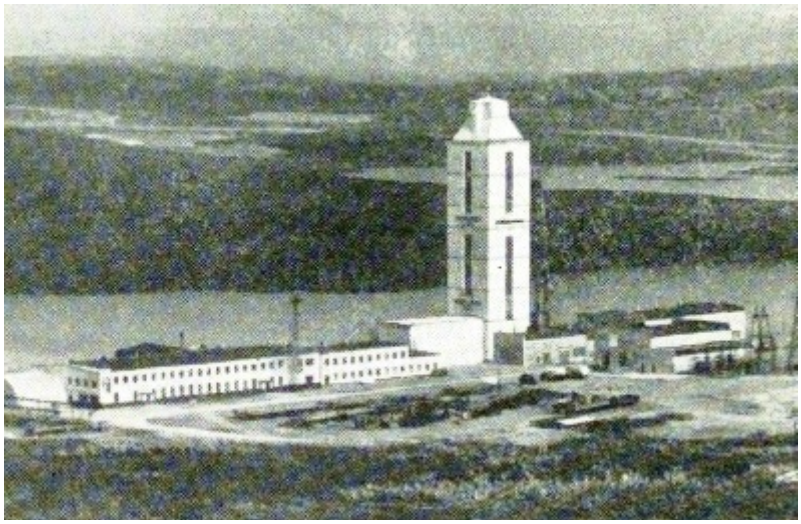

Fig.2 General view of Kola rig.

2.2 Geological description of the location

The geological pattern of the location of the well is composed by ancient differently metamorphosed crystalline formations which are typical representatives of Precambrian complexes of the Baltic shield.

High interest of the geologist to this location caused by the existence here of copper-nickel formations deposited among the sedimentary rocks of Proterozoic complex. Therefore, the main volume of investigation work was concentrated in the most perspective zone of development of sedimentary rocks.

Pechenga district is a north-western side continuation of Central Kola's geotectonic synclinoric zone. This zone limited by the large longitudinal fractures from the south and from the north. Among the common within the area Precambrian formations the following age complexes distinguished:

- Proterozoic (formed by volcanogenic supracrustal beds of Kola karelides zone);
- Archean (rocks represented by tectonic blocks formed by fold-dome tectonical structures) [2].

Below the Archean series at the depth of 7 km expected the granulite-basite thickness of indefinite depth of several kilometers. Each of these complexes has their own structural features, metamorphism, magnetism and ore occurrences.

It is important for as to review the common picture of geological structures and determination methods used. It helps on a par with pressure and temperature conditions to understand the level of stresses in the rocks and evaluate the risks and technical decisions selected for the drilling. At the same time we are not going to very detailed in the geological description as it deserved special focused huge amount of work and not particularly subject of the thesis.

At the figure 3 shown the simplified schematic section of the continental Earth's crust at the location of the Kola rig. It is a simplified prognosed pattern restructured according to the data of deep drilling. As we can see on the schema there are some several wells drilled some kilometers away of the Kola rig. The fact is that by this time Soviet Union and United States had a several number of the well drilled at the depth of 7-9 km in the sedimentary rocks with the purpose of investigation of the oil and gas reservoirs. These wells were projected in the sedimentary basins and as a rule opened the same layering pattern which comes out on the surface at the continental border of the basin. That's why this type of wells was less affective in terms of investigation and understanding of deep regions of the crust.

2.3 Geological structure of the well according to geophysical investigation

Section characteristics of the Kola rig based on the complex study of coring material and geophysical investigation of the near well surrounding area. Figure 3 shows schematic section of the Earth's crust at the location of the rig. In addition to the seismic data the following main geophysical methods has been used:

- caliper logging
- acoustic logging
- gamma logging
- spectra-gamma logging
- gamma-gamma density logging
- neutro-gamma logging
- neutro-neutro logging
- magnetic logging
- electric logging
- thermo-logging

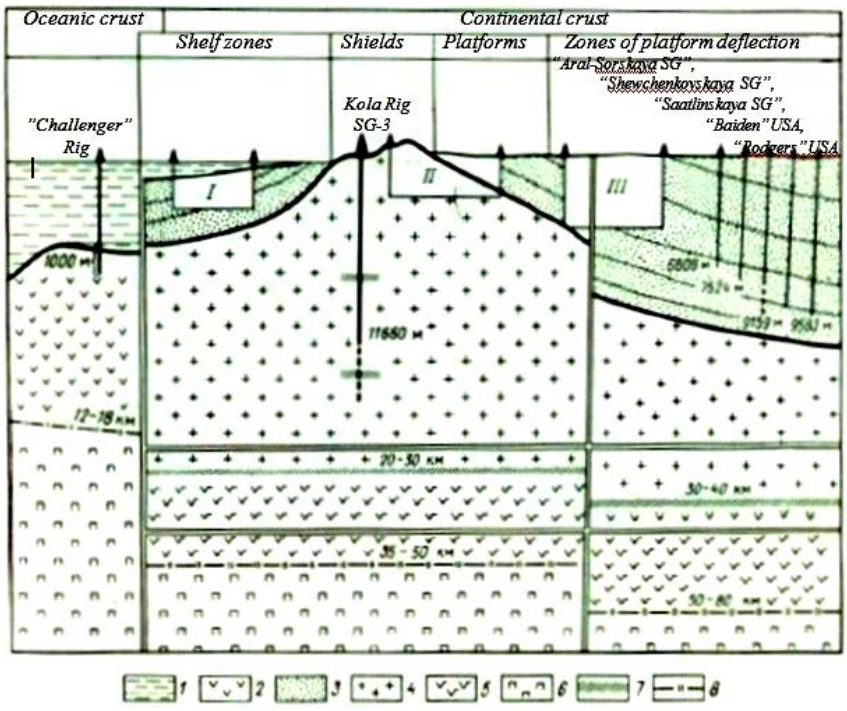

Fig.3 Schematic section of the Earth's crust at the location of the Kola rig.

Exploration drilling contours of the depths: I – in the shelf zone; II – for investigation of solid minerals; III - oil and gas wells. 1 – hydrosphere of the Earth; 2 – oceanic basalts; 3 - sedimentary and sedimentary-volcanogenic Phanerozoic formations (age of 500 mil.); 4 - Precambrian crystalline rocks of granite layer (age of 1000-3000 mil.); 5 – continental basalts formation; 6 – mantel formation; 7 - high-speed layers – Conrad border ($v_{p\text{-}wave}$=6,6-6,8 km/s); 8 – Mohorowich border or Moho ($v_{p\text{-}wave}$=8,0 km/s).

By well known method of logging parameters comparison the types of rock was identified and the depth of every certain layer was obtained. Geophysical data of real drilling showed significant differences with predicted in advance and projected depths of the rock borders.

The well SG-3 was planned to cross volcanogenic formations of Pechenga complex and at the depth of 4700 m enter the Archean gneisses. At the depth of 7-8 km was planned to enter the high-speed granulite-basite layers [2]. But the actual cut along well was different from the predicted (Fig. 4). Later these uncertainties became the reason for the special approach of

drilling process using so called protection casing and also special challenge related to the casing design. We will devote the attention to the method used for drilling in a later chapter.

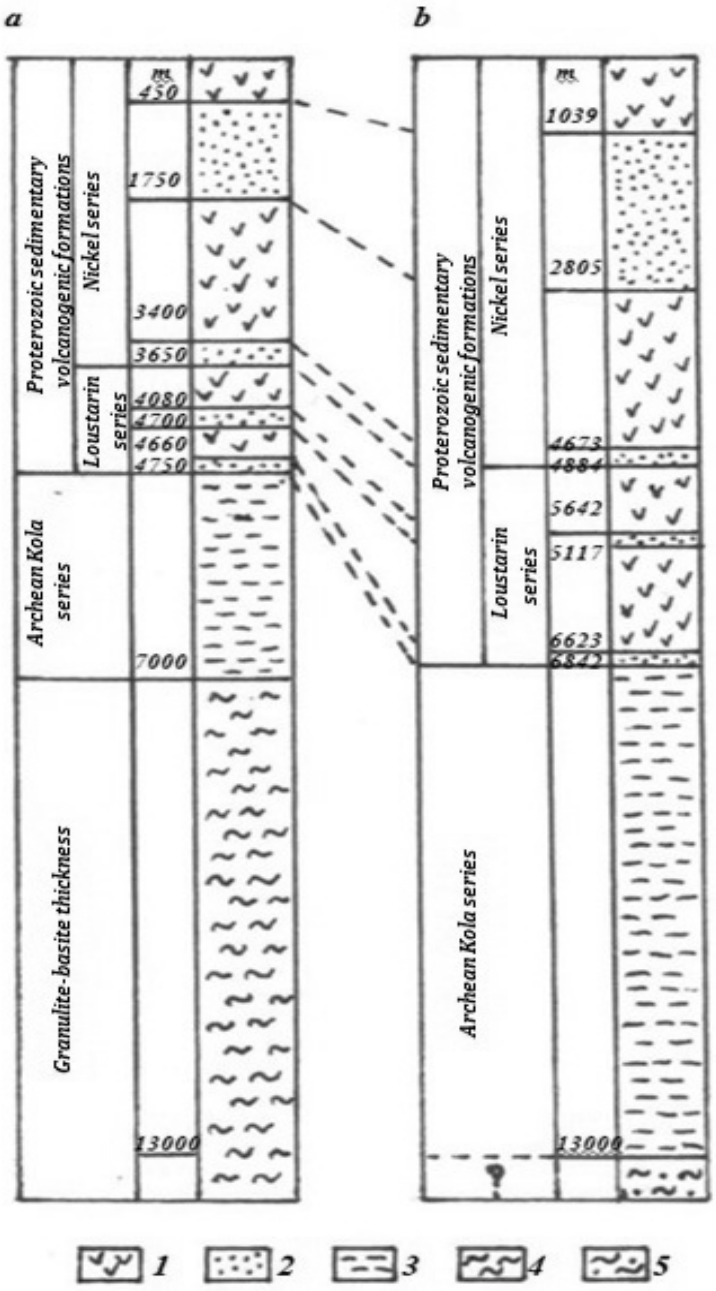

Fig. 4 Comparison scheme of geological vertical intersection of the Kola rig strata (a- according to the seismic data; b – according to the actual drilling data).

1 - effusive formations of basic structures (diabasic porphyries, metadiabases); 2 – sedimentary formations; 3 - gneisses and amphibolites; 4 - granulite basalts; 5 – highly metamorphosed gneisses and amphibolites.

2.4 Technological problems of geophysical investigations

The aim to achieve a great depth of drilling required solution of a range of principally new technological problems with the help of geophysical methods. Among these problems was evaluation of well bore open hole stability and condition study of drill-pipes at the huge temperatures and pressures. Obtained information was used for justification of optimal drilling modes and solution developing in the cases of complications and its liquidation. As previously

mentioned, geophysical study and logging methods created necessary informational supply of drilling work.

A particular difficulty became a reliable transfer of information through the cable of huge length. With increasing length of borehole cable, which been used at that time for logging tools also increased the electrical capacitance and resistance of cable wires and consequentially current lost. That leads to reduction in the intensity of transmitting signals. Was developed special operational control system to prognose and avoid of accident situations and control of operational cable parameters. It includes definition of interval and integral deformations in the cable cross section frequency of cable rotation and cable tension. An electrical property of the cable and its insulation was monitored.

Cable parameters observably changes during tripping cable down to the well on the big depth. Thus, certain difficulties occurred during the fitting of rig and borehole elements of equipment with elongated communication line. Was required a number of new circuits instrumental and constructive solutions.

During the geophysical investigations and explosions work in the borehole was used serial self-moving elevators (PK-4 and PKS). In the second phase of SG-3 project the condition of geophysical investigations were greatly complicated. Abrasive wear of the cable and contact friction force along the borehole wall sharply increased. There was an increased jamming risk of the cable and devices in the flumes and cross-sections of the open hole [2].

With the purpose of protection of the cable from the wear and jamming prevention also reducing operating loads on the cable and elevators was developed the technical tools which secured protection of the main part of the cable by the section of drill-pipes. Before insertion of the geophysical assemblage first in the well tripped a section of drill-pipes with installed funnel in the down part. This section cover whole open hole except the investigation interval (up to 700-1000 m). All developed borehole devices has streamline shape and diameter smaller then funnel’s output.

For example cable of smaller cross-sectional diameter together with connected device after launching it down to the depth of 6000-7000 m was fixed on the orifice of the open hole. The free end of this cable section was connected to another cable section of bigger cross-sectional diameter. Rerolling of cable was done if needed and necessary tension created.

Described technology of geophysical investigation developed for SG-3 made possible process of measurement on the record depths and completely excluded difficulties of drilling by reason of cables and devises left in the borehole.

3 Drilling issues of Kola ultra deep well

One of the most common difficult problems of deep drilling is a lack of accurate information about the geological rock sections. Actual geological and technical conditions of the well not always can be complied with predicted. Insufficiently justified design and construction of the well may generate a number of serious complications. Based on the experience of deep drilling, the geophysical data as a rule formed out of indirect methods of geological study of the deeper layers, comparison with the closely drilled wells and predictions. Seismic in this case not always can give sufficiently accurate data.

As an example in a 7000 m deep well “Djarly” drilled in the Azerbaijan Miocene sediments was supposed to reach at the depth of 3500 m but in fact this sediments was open at the depth of 2875 m [2]. Analysis of deep drilling experience shows that uncertainties in the depth predictions increases with increasing depth. What are more errors in the depth of stratigraphic layer often exceed the projected casing shoe intervals.

3.1 Theoretical method of drilling ultra-deep.

Due to insufficient reliable information about the species of the section there is a difficulty in a choosing of the optimal design of the well. The core problem here is the absence of initial true data for correct justification of the casing’s quantity, it diameters and depths of the casing shoes. Very often the information about the rock and geological environment obtained by seismic turns out to be unreliable. Luck of initial data leads to extensive complexity borehole design.

In case of super-deep drilling the telescopic borehole design strategy can be a solution in the complex geological environment and technological conditions of drilling. However the approach of detailed designed well turns out to be practically unfeasible for implementation at significant depth. For example in the case of KTB scientific borehole in Germany the initial diameter was 28 in (711 mm) and the last casing string with a diameter of 5 and ½ in (140 mm) was run to the depth of 9031 m. The small diameter of the last casing became the limiting factor preventing the further deepening of the well in this case [7].

For drilling of Kola ultra deep well was developed a special approach which provided possibility to correct construction of the well directly during the drilling process according to the actual geophysical characteristics of the newly drilled layers. This method was developed by so-called Problematic Laboratory for Drilling on the Mantle (Russia) and became the solution for optimization of the well design in the cases with insufficient information about the geological layers. Let us call it “blind drilling concept”.

The essence of the method based on the fact what during the projecting of the well not the whole structure of the well is justified but only its upper part where the geological information is most reliable. Usually it related to the depth of the first and second casings. The diameter of the first casing selected as big as possible in case of appearance of any complications in the dipper drilling and created capacity for us to install a high number of the casings.

After tripping down and cementing of the first or second casing the borehole is not drilled further as well known from traditional drilling of the oil wells. In the stationary cemented casing another one casing of smaller diameter (so-called protection casing) is tripped down and fasted on the surface with the possibility to turn it and remove. Next the pilot hole drilled with the small diameter which provides best technological and economical parameters.

The pilot hole drilled in combination with very careful geophysical measurements and study of conditions of the newly opened layers and possible detected difficulties. In case of apprized complicates, which is possible to avoid only using an additional casing, the pilot drilling is stops and the protection casing is pulled out. The pilot hole widens by bigger drill bit diameter and the next stationary casing tripped down and cemented. Drilling of next pilot hole repeatedly continued with additionally installed new protection casing [2].

Diameters of widening boreholes and casings selected according to the achieved depth, length of drilling interval left and predictions of it possible complexibility.

This method has following advantages:

- provided maximum simplification of the design of the well;
- unification of drill bits, borehole assembly and drill pipes;
- provided protection of stationary cemented casings from the wear;
- improved condition of wellbore cleaning and pressure regulation by using hydraulic channel between stationary and protection casings [2].

Described drilling technology was selected as the most effective for the crystalline rocks on the big depths where mining and geological conditions are poorly understood.

3.2 The theory and reality of drilling SG-3

Project of drilling SG-3 was divided on two stages. First part of drilling was carried out with a standard commercial rig installation of Russian producer called ”Uralmash 4E” with 2000 kN carrying capacity. It’s allowed to reach the maximum possible depth with this rig up to 7262 m.

First of all the surface casing with 28 in (720 mm) diameter was installed down to 40 m. After this 8 and ½ in (215,9 mm) diameter hole with continuous coring operations was drilled down to the depth of 5369 m. Where has been met some problems related to borehole wall instability in cavernous zone at the depth of 1800 m. It can be very good observed at the caliper log later. The reaming was forced and one more additional casing of 12 and ¾ (324 mm) diameter was set up to the depth of 2000 m. Later in 1975 the open borehole with the same diameter of 8 and ½ in was cored down to the maximum achievable depth with this rig.

On the figure 5 shown the sketches of pre-designed (a) and actually drilled (b) SG-3 well. It eloquently indicates how untenable can be predicted designing in the case of super-deep drilling.

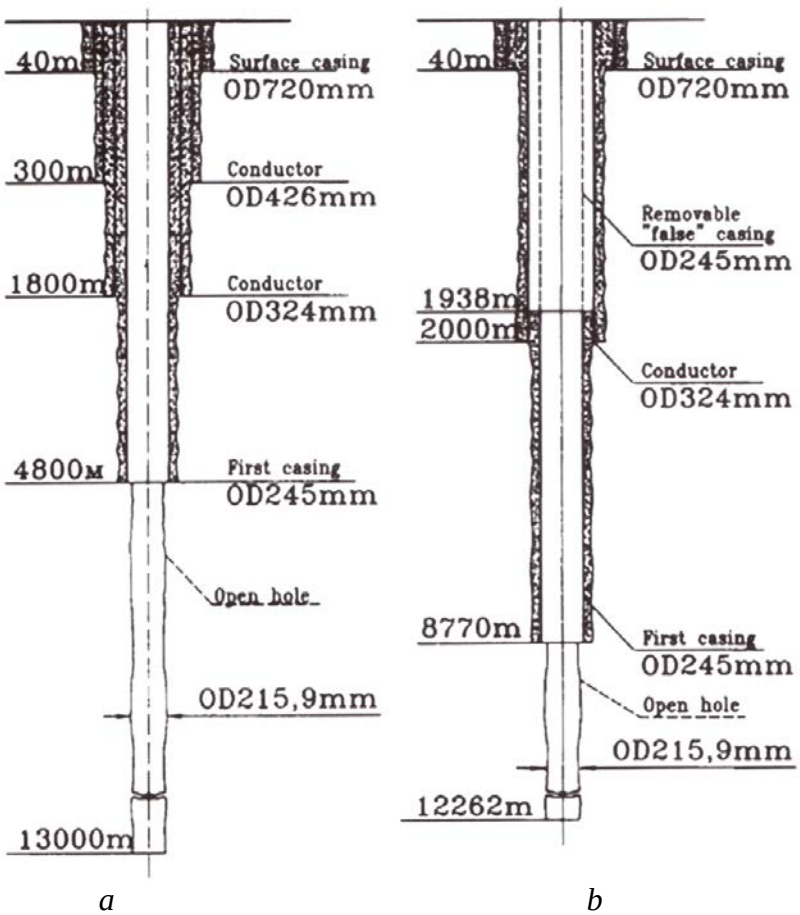

a *b*

Fig. 5 Pre-designed SG-3 (a); actually drilled SG-3 (b) [7].

After approximately one year a new rig installation called “Uralmash – 15000” with 4000 kN carrying capacity was installed and drilling continued with the same bit diameter. In 1983 the depth of the well reached a record mark of 12000 km and the open borehole extent made up 10000 m. 85 % of penetration was conducted with coring tool and only about 40% of core material were recovered. The static temperature at this depth after 24 hours without any mud flow was recorded at the level of 220°C.

Next year a complete set of scientific research logging in the open borehole was fulfilled and drilling was continued. In the next run during the tool pull out of the hole the BHA was stuck at the depth of 12066 m. All attempts to prevent the stuck drill string by pulling out were useless. Finely external load of tension resulted in the breakage of drill string body at the depth of 7 km. Unfortunately the breakage occurred in the cavernous zone in the place where the top of drill string could be deflected and as a result all attempts to connect the drill string with the fishing tool were in the vain. In this difficult situation was made the solution to ream the borehole up to the depth of 8 – 9 km by the diameter of 11 and 5/8 in (295 mm). The aim was to widen the hole for the casing string with diameter of 9 and 5/8 in (245 mm) to overlap the unstable cavernous interval in the upper layers.

At the depth of 7000 m where the broken drill pipe remained in the borehole and spontaneous sidetracking took place. The deviated part of the pipe played here the role of sidetracking choke. New bypass borehole was continuously drilled further with the same diameter of 11 and 5/8 in down to the depth of 8770 m. After 8 and ½ in (216 mm) casing installation drilling was continued and in the 1990-th borehole reached 12262 m [7].

The TMD of Kola well had the record of drilling until the end of century but TVD of SG-3 is still remains the deepest record of world drilling practice. The further drilling operations were canceled because of luck of financing and reduced practical interest from the authorities. So far the borehole became a scientific geo-laboratory for realization of relevant geophysical research.

3.3 Stability of open borehole.

The success of bringing the well to a projected depth determined by the optimality of the wellbore structure and especially maximum allowable depth of each open hole drilling. In this case becomes very important to save wellbore stability and to make right predictions of locations with possible caving and collapse of the borehole wall. This information gives opportunity to manipulate and manage the processes flowing in the loop of open borehole. It became important for us to describe concept of wellbore stability and include additional risks of borehole collapse and corresponding additional stresses on the drill pipe on the certain depth wile modelling the drill string design.

3.3.1 General about wellbore stability

Factors on which depends stability of wellbore are varied but contingently it can be divided on two groups:

- geological (strength characteristics of rocks, their structure, type of formation and bedding, gravitational and tectonic stresses);
- technological (geometrical parameters of the well, it orientation, type and density of the drilling mud, drilling method, descent depth of intermediate casings, technique of lowering and lifting operations) [2].

Typically borehole enlarges with time. This collapse phenomenon has a time dependent characteristic. Possible problems that can occur cased by hole enlargement are difficulties in removing rock fragments and drilled cuttings, or reduced quality of cement placement behind the casing. In a sense tight hole and borehole collapse are similar events. If in first case the hole may yield, in another case later abrupt failure may occur [3]. Collapse of the hole is the most costly

problem during drilling and in particularly case of drilling ultra deep well it can become a crucially serious on the big depth.

3.3.2 Basic theory of collapse mechanism offered for Kola crystal formations

The core elements of any borehole collapse analysis are three stress components acting on the wellbore. In our traditional understanding of the analysis of oil wells drilled in a sedimentary rock there are three normal stress components acting on the borehole wall (fig. 6). In the simplest form for a vertical well they can be defined as follows [3]:

Vertical stress: $\sigma_z = overburden\ (constant)$
Radial stress: $\sigma_r = P_w = borehole\ pressure$
Tangential stress: $\sigma_\theta = 2\sigma_a - P_w$, where $\sigma_a = estimated\ average\ horizontal\ stress\ gradient$
Pore pressure: P_o

Formation pore pressure is defined as the pressure exerted by the formation fluids on the walls of the rock pores. This pore pressure supports a part of the weight of the overburden stress, while the other part is taken by the rock grains [4].

The effective stress principle says that the total stress is the sum of the pore fluid pressure and the stress taken up by the rock matrix itself. Considering the failure of the rock matrix, we have to use effective stresses written as follows [3]:

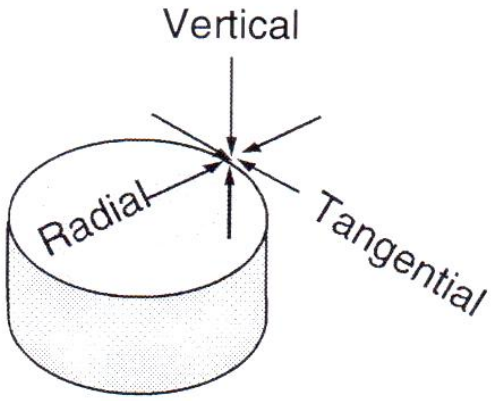

Vertical effective stress: $\sigma_z' = \sigma_z - P_o$
Radial effective stress: $\sigma_r' = P_w - P_o$
Tangential effective stress: $\sigma_\theta' = 2\sigma_a - P_w - P_o$

On the figure a shows three principal stresses acting on the borehole wall.

In our case we are dealing with crystal formations on the big depth, where pore pressure difficult to predict by geophysical methods.

Fig. 6 Principle stresses acting on the borehole wall.

By the crystal formations we are meaning igneous rock or metamorphosed rock having crystal structure. We could possibly apply to the classical effective stress principle using normal formation pore pressure (hydro-pressure) as assumption. This is when the formation pore pressure is equal to the hydrostatic pressure of a full column of formation water [5]. Normal pore pressure is usually of the order of 0,465 psi/ft.

As a basis for Kola ultra deep well the following model described below was taken by geo-engineer. Gravitational field at any point is characterized by weight of rock lying above (overburden weight) and associated with the peculiarities of the geological structure of the strata.

Vertical stress gradient can be written as [2]:

$$\sigma_z = \sum h_i \gamma_i \qquad (3.1)$$

Where h_i - thickness of layer *i*; γ_i - specific weight of the interval *i*.

Horizontal components at any point of elastic anisotropic body:

$$\sigma_x = \sigma_y = \xi \sum h_i \gamma_i \quad (3.2)$$

According to opinion of many researchers even the most durable crystal formations gradually transformed into a plastic state with increasing pressure and temperature at a depths of 10-s of kilometers (ν close to 0,5 and ξ close to 1). In this case hydrostatic stress distribution occurs: $\sigma_x = \sigma_y = \sigma_z$ [6].

Here $\xi = \nu/(1-\nu)$ - coefficient of lateral thrust (shows a part of active load made by reactive stresses in conditions when deformation in perpendicular plane to active force is absent); ν - Poisson's ratio.

Another component - tectonic component of the field of stresses is different from gravitational component and has significantly greater complexity. Direction of the forces depends of orientation of tectonical structures and deep faults. In general the main stresses caused by tectonic component can be written as follows [2]:

$$\sigma_x = F_T;\ \sigma_y = \psi F_T;\ \sigma_z = \chi F_T \quad (3.3)$$

Here ψ and χ - horizontal and vertical factors of the tectonic force F_T. Wherein $\xi > \chi \geq 0$ and $\xi > \psi \geq \nu$.

Emersion of tectonic stress established experimentally. These stresses at shallow depths often exceed the gravitational. There is an assumption that excessive horizontal stresses in the upper crust formed as secondary effect of vertical uplift of tectonic blocks.

Equations that characterize field of stresses in the isotropic media near the borehole wall including pressure of the drill mud offered as follows [2]:

$$\sigma_z = \gamma_f H \quad (3.4)$$

$$\sigma_r = \xi \gamma_f H \left(1 - \frac{r^2}{a^2}\right) - \gamma_m H \frac{r^2}{a^2} \quad (3.5)$$

$$\sigma_\theta = \xi \gamma_f H \left(1 + \frac{r^2}{a^2}\right) + \gamma_m H \frac{r^2}{a^2} \quad (3.6)$$

Here $\sigma_z, \sigma_r, \sigma_\theta$ - vertical radial and tangential stresses respectively; γ_f, γ_m – specific weight of formation and drilling mud respectively; H - depth; r – radius of borehole; a - distance from the center of the borehole to the point of measurement.

Formations around the SG-3 well characterized by varying degree of anisotropy. To take into account anisotropy, we can by using the factor indicating the change in the stress condition [2]. Not going too deep into that we just mention that average level of stress component was decreased approximately by 20%.

3.3.3 Kola well collapse evaluation

According to the data released in [2], for the formations of Kola region destruction of wellbore is absent if between actual stress (assumed σ_θ as a maximum stress) and yield strength of rock σ_Y there is a relation: $\sigma_\theta < 0{,}3\sigma_Y$.

Flaking, foliation peeling, chipping and caving can occur at $\sigma_\theta = (0{,}5 \div 0{,}8)\sigma_Y$.

Intensive caving and collapse can occur at $\sigma_\theta > 0{,}8\sigma_Y$.

Therefore stresses corresponding to the range of $(0{,}5 \div 0{,}8)\sigma_Y$ may be considered sufficient for the loss of wellbore stability [2].

Experimentally determined value of yield rock strength of crystal formations listed below (in MPa):

Shales 103-231

Amphibolites 140-287
Biotite gneisses 150-269
Epidote-biotite gneisses 194-268
Granites 215-298
Porphyrites 160-244
Basalts 217-309

In the table 1 collected calculation completed for the conditions of drilling with water based mud with density of 1.15 g/cm^3 shows that following hoop stresses will arise in the wellbore depending on the drilling depth [2].

Table 1 Tangential stresses in the borehole wall depending on the depth.

Maximum stress ($tangentional\ \sigma_\theta$)	**Depth of the wellbore, m**					
	4000	6000	8000	10000	12000	15000
Max stress for isotropic formation, MPa	39,0	59,0	78,5	98,0	117,5	147,0
Max stress for anisotropic formation, MPA	31,2	47,2	60,8	78,4	94,0	117,6

Out of the data presented in the source [2] we can make several conclusions concerning wellbore stability. From the figure 4 we can see the following formations:

- porphyries formations from 2800 m depth to 6600 m ($Assuming\ 0{,}5\sigma_Y = 0{,}5 \cdot 160 = 80\ MPa$);
- sedimentary rocks at 4700 m, at 5700 m and at 6700 m ($Assuming\ same\ for\ shales\ 0{,}5\sigma_Y = 0{,}5 \cdot 103 = 51{,}5\ MPa$);
- gneisses and amphibolites from the depth of 6800 m to 13000 m ($Assuming\ 0{,}5\sigma_Y = 0{,}5 \cdot 194 = 97\ MPa$).

Here we assume the lowest values of yield rock strength as a basis for evaluation of rock formation and a coefficient of 0,5 of yield rock strength sufficient for the loss of wellbore stability. Assuming also values of tangentional stress for isotropic formations as it gives a highest values and is a worst case scenario.

Combining all information we can generate the plot and try to predict the depths of drilling with most probable loss of stability. At the figure 7 we can see the interpretation of the predicted loss of wellbore stability at the condition of $\sigma_\theta = 0{,}5\sigma_Y$ if using water based drilling mud with density of 1,15 g/cm^{3}as been mentioned above. The graph shows that during the drilling at a depth of 5700 m, 6700 m as well as deeper then 10000 m complications may occur. At these depths would be worth to increase the density of the mud solution to the maximum possible values to compensate for the resulting tangential stresses across the cylindrical hole.

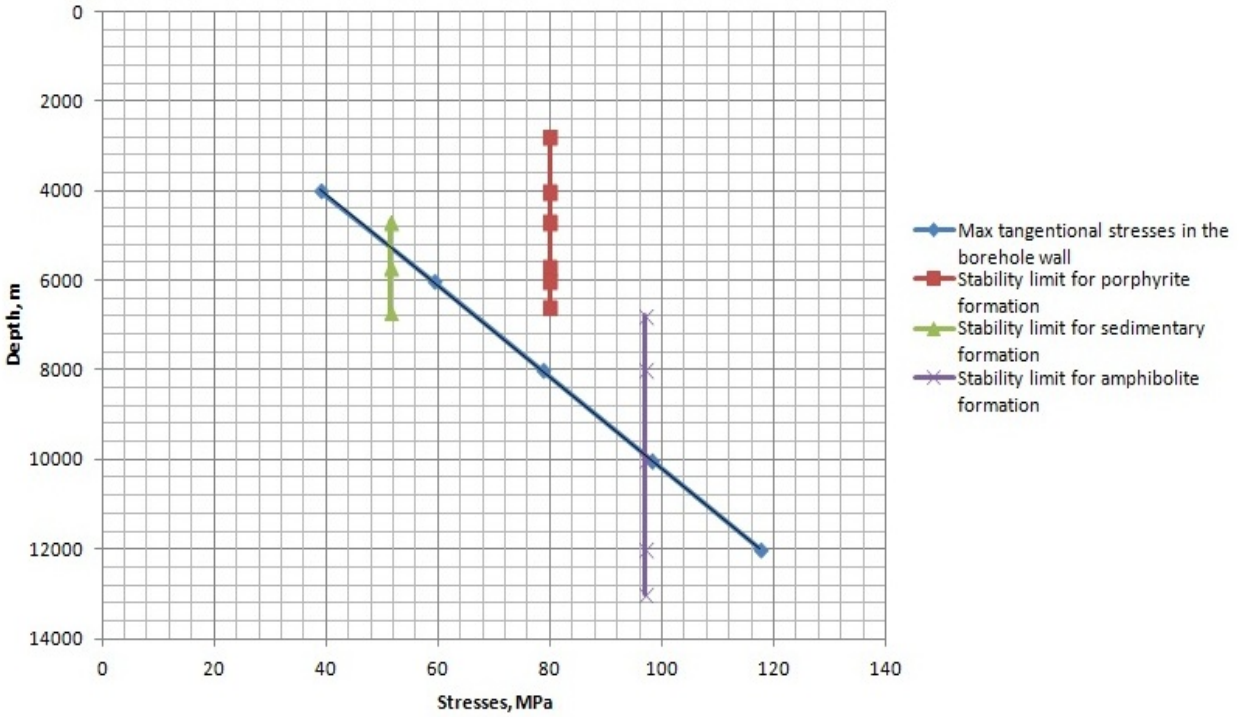

Fig. 7 Wellbore stability prediction based on condition of $0{,}5\sigma_Y$ *for main types of formations on the actual depth.*

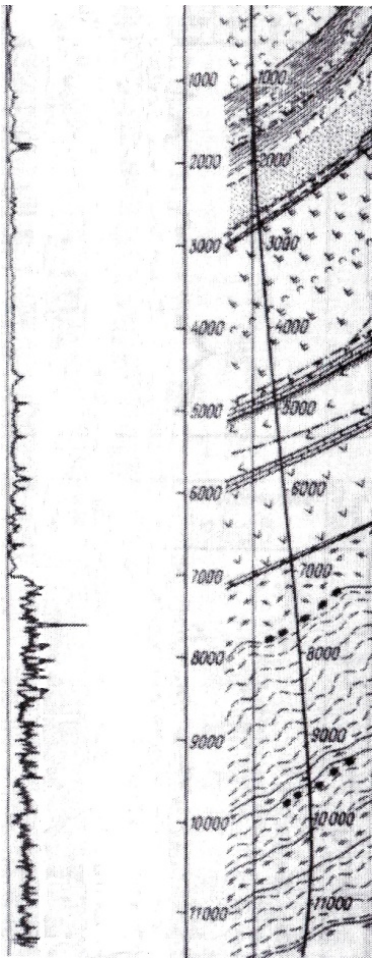

Interesting result of calliper log data of actually drilled SG-3 well was given in the source [2] (fig. 8). As we can see stability problems stars to appear at the depth of around 5000 m with some shocks at the level of 6000 m. Later at 7000 m and deeper stability gradually decreases again.

This picture, with some level of uncertainty, is mostly corresponding to our prediction built on the theory proposed in source [2] and based on stratigraphic pre-drilling intersection on figure 4.

In addition to static loads the dynamic loads occur on the contour of the well associated with round-trip operations and wash out of the well. The strength of the rocks can also be affected by the temperature of the surrounding area and its change during the circulation of mud. In this case cyclic alternation of the temperature and other hydro-dynamic loads can cause fatigue failure of the formation.

Later in our work as been mentioned earlier we will take a look at the risks of borehole collapse and corresponding additional stresses on the drill pipe on the certain depth wile modelling the drill string design and correlation with field data. Out of the story of drilling the SG-3 it became clear that collapse problems, temperature and yield limits of materials became the main factors of suspension of drilling and completion of the project on the level of 12 262 m.

Fig. 8 Calliper log data of drilled well SG-3.

3.4 Temperature condition in the borehole.

The process of deepening of borehole basically consists of set of operations. Each of them includes tripping up and down operations; intermediate washes; drilling itself and downtimes. All of these operations induce the change of thermal conditions in the borehole. There are factors that make significant adjustments in the heat flow distribution in the borehole. Among them increase in temperature of rock body with the depth and variable value of heat transfer from the rock body to the mud fluid and from the mud to the drill-string.

Drill-string in the Kola well consists commonly of light alloy aluminium drill pipes and its strength has direct dependence of thermal conditions. Dynamic change of temperature during the operation necessitates careful completion of drill-string assemblage taking into account bordering strength condition of alloying material.

To get the true values of temperatures during the drilling and mud circulation of SG-3 was special experimental work conducted directly by measurement of autonomous constructed thermometers. The temperature was measured at the depths of 6015, 6275, 6950 and 10909 m. In the table 2 presented the data of measured static and dynamic temperatures and on the figure 9 shown the plot built according to the table data. Dynamic temperature was measured at the steady volumetric mud flow of q=32 l/sec [2].

Table 2 Dynamic and static temperature gradients.

The depth of the measurement, m	**Static temperature, ^{o}C**	**Dynamic temperature, ^{o}C**
890	17.6	36.3
2990	38.1	51.2
3470	44.5	53.4
3960	51.8	59.0
4540	61.4	65.1
4850	68.0	69.0
6015	89.2	82.5
6350	95.2	88.0
6510	99.5	90.6
6950	106.6	95.5
7800	123.0	107.0
8230	131.0	113.0
10425	172.8	141.0
10909	183.0	146.6
11340	193.8	152.4

The analysis of thermometry data showed that difference in temperatures of down flow and up flow of drill mud not exceeds 40^{o}C both during the washing and drilling operations. Distribution of temperature field along the depth with the high level of veracity obeys to the linear law. Equilibrium zone of temperature gradient in the borehole at the volumetric flow of q=30~40 l/sec is at the depth of 5000 m. Time needed for recovery of temperature regime in the borehole not exceeds 50 hours. The recovery speed of thermal field indicates that the radius of thermal influence in the lower part of the well is gradually lower than in the upper part (higher than 5000 m). Temperature measured at the drill bit is closed to the calculated using geothermal gradient (around 17^{o}C) [2].

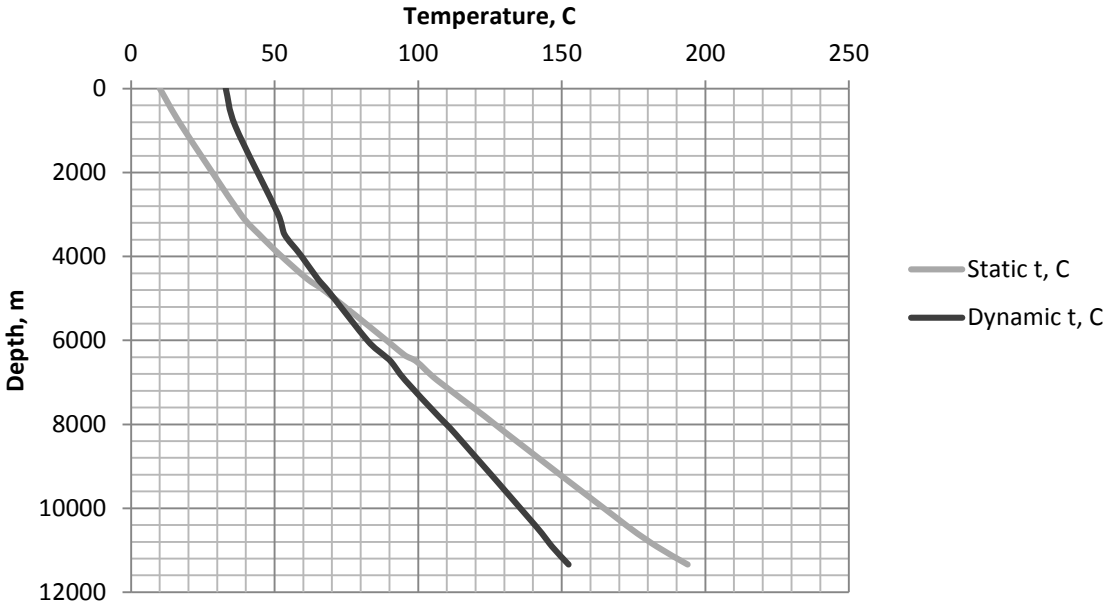

Fig. 9 Dynamic and static temperature gradients.

The plot showing temperature recovery in the borehole on the depth of 11000 m presented on the figure 10.

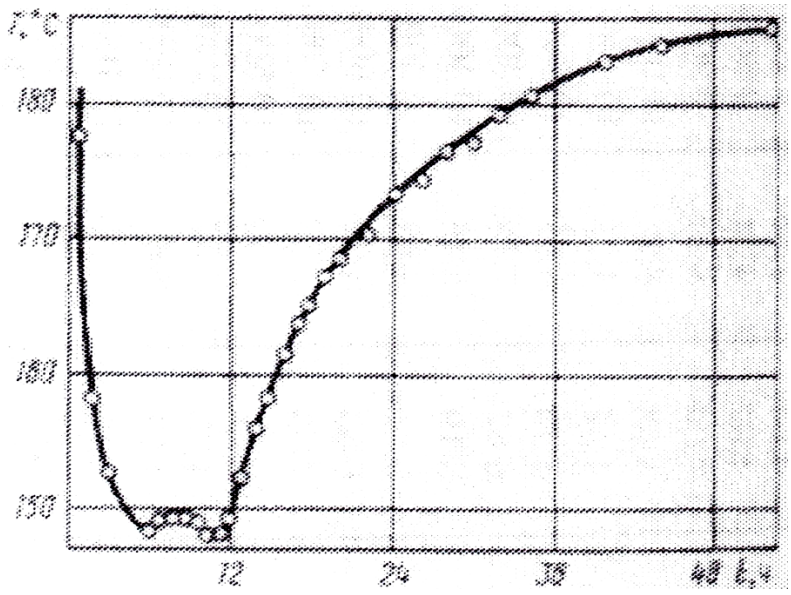

Fig. 10 Recovery of the temperature in the borehole of SG-3 at the approximate depth of 11000 m [2].

4 Drill string design.

This section contains wide description of analytical friction model of drill string applicable primary for the petroleum wells. Such a model can be absolutely suitable for our super deep well drilling since it is based on the common cylindrical well friction theory and applicable for all kinds of wellbore shapes such as straight sections, build-up bends, drop-off bends, side bends or those combinations.

Our main purpose is to use provided theoretical model for simulation of case scenario of drilling Kola ultra-deep well where light aluminum drill string were used in a harsh temperature condition. Our object of interest is to provide of theoretically based drill string load scenarios and clear illustrations of results using Excel plotting tool. Upon the history and available data of drilled SG-3 well we will try to analyze the condition of drill string proposed by the drillers, look at the limiting factors and achievable depths of drilling and give the conclusions about possible resource for improvement of drilling strategy.

4.1 Theory of drill string mechanics.

According to the theory proposed in the source [3] the entire well can be modeled by two set of equations, one for straight wellbore sections and one for curved wellbores. By separating gravitational and tensional friction effects we will provide a simple frictional model. The second one is based on the absolute directional change of well path (dogleg of the wellbore). We will review a 2-dimensional well, a 3-dimentional well and later consider combined tension load and rotation in the more realistic 3-dimentional well.

4.1.1 Loading mechanism.

First of all let us take a look at the effects which inclination of wellbore has on the loading parameters. On the figure 11 an inclined pipe segment is shown with the axial and normal weight components acting on the bit. The loading caused by external and internal fluid pressures is independent of the orientation of the pipe segment. The weight of the pipe, however, is no longer axial and weight can be decomposed into an axial and a transverse component.

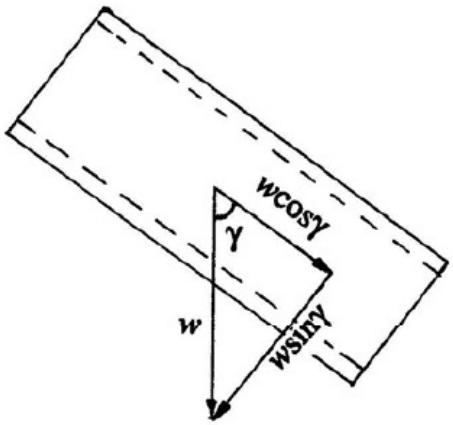

Fig. 11 Axial and normal weight component acting on the pipe segment.

When pipe is moved namely the normal to the pipe wall component gives the rise to friction force. The weight of the entire drill string is the sum of all axial loads throughout the string. For the pipe segment presented on the figure 11, the effective axial load is:

$$w(\gamma) = w\cos\gamma \qquad (4.1)$$

The normal force on the borehole wall is:

$$n(\gamma) = w \sin \gamma \tag{4.2}$$

If the pipe has a length of L, a projected height of true vertical depth D_{TVD} becomes:

$$D_{TVD} = L \cos \gamma \tag{4.3}$$

It called “the projected height principle” [3]. Inserting this expression into equation 5.1 results in the following expression for the axial component of the pipe weight:

$$w(\gamma) = \left(\frac{w}{L}\right) D_{TVD} \tag{4.4}$$

Equation 4.4 shows that the axial pipe weight is equal to the unit pipe weight multiplied by the projected height. This gives the static pipe weight regardless of well path and inclination. Friction forces must be added or subtracted when the pipe is moved in the borehole or pulled out of it.

4.1.2 Pipe weight in the mud solution

The load on the hook in the static condition is equal to the buoyed pipe weight multiplied by the projected vertical height of the well, regardless of wellbore orientation. Thus, a vertical well has equal static hook load as deviated well with the same true vertical depth or projected depth [8].

Buoyancy factor must be always taken in consideration while modeling loads on the drill string. The buoyancy effect is constant regardless of pipe orientation, but the effective string weight in the mud-filled well should be reduced by multiplying unit pipe weight by buoyancy factor. Buoyancy factor defined as follows:

$$\beta = 1 - \frac{\rho_0 A_0 - \rho_i A_i}{\rho_{pipe}(A_0 - A_i)} \tag{4.5}$$

Where A_0, A_i - outside and inside pipe area; ρ_0, ρ_i - density of inside and outside mud respectively; ρ_{pipe} - density of the pipe body.

Equation 4.5 most commonly used in cementing operations, in case of sufficient difference between the inside of string and the annulus [3].

If the fluid density of inside and outside of the drilling pipe is equal, the buoyancy equation becomes:

$$\beta = 1 - \frac{\rho_0}{\rho_{pipe}} \tag{4.6}$$

Equation 4.6 is most widely used during calculating of weight of drill string while drilling. In our modeling we will also assume the same mud density inside and outside the drill string despite the fact that we are dealing with the long distances and gradual adjustment of mud weight can take place often. Unfortunately this kind of detailed information is not provided in any sources. So anyway it will not sensitively affect the calculations and difference in mud weight can be assumed negligible.

During well intervention operations, the wellhead may be shut in and an annular pressure applied. The same buoyancy equation applies, but one must add a reactions caused by the annular pressure [3]. In our case we will not assume similar scenario.

4.1.3 Three-dimensional orientation of wellbore

To get the general wellbore orientation two main slope parameters must be computed. They are dog-led (DL) and dog-leg severity (DLS). The dog-leg is the absolute change of direction in the space media and the dog-leg severity is the derivative of dog-leg.

To compute DL and DLS two main parameters basically measured during standard drilling operation: well bore inclination - α (measures deviation of wellbore in the vertical plain) and azimuth – ϕ (measures deviation of the wellbore in the horizontal plain). First of all we have to find absolute change in direction θ:

$$\cos\theta = \sin\alpha_1 \sin\alpha_2 \cos(\phi_1 - \phi_2) + \cos\alpha_1 \cos\alpha_2 \quad (4.7)$$

The dog-leg determined from the following equation:

$$DL(^\circ) = \frac{180}{\pi}|\theta(rad)| \quad (4.8)$$

Indexes 1 and 2 refers to the two fixed spatial survey measurements of drill bit location, or with another words to the start and end of wellbore section. Dog-leg severity determined from the equation:

$$DLS = \frac{DL(^\circ)}{\Delta L(m)} \quad (4.9)$$

Here ΔL - defined as a distance between two points of measurements 1 and 2 [3].

Concerning SG-3 well As well known from the sources, Kola well has been projected as an ideally vertical well with the main purpose to reduce friction and reach a maximum allowable depth of 13000 m and deeper. But as we know from the history of drilling the sidetracking occurred at the depth of 7000 m generating as a minimum of one build-up and one drop-off section. So for our modeling can be reasonable to assume those sections with various angles between 10^o and 15^o both in wellbore inclination and in azimuth. In addition if we look at the figure 8 where the well path can be observed, then we can see that our well starts to build up angle of approximately 5^o (can be assumed in both planes – wellbore inclination and azimuth) at the depth of 2000 m. So, we will take a look more precisely at different variations and out-coming results in the modeling part of the thesis and will try to find the assumption, which most closely will fit the historical reality. Furthermore we will try to analyze through this the drilling experience of SG-3 and prognose the achievable drilling prospects of super-deep drilling out of the results of implemented modeling tool.

4.1.4 Drag and torque in the spatial friction model

Following model assumes so called “soft drill string”. This implies that pipe bending is so small that bending stiffness can be neglected [3]. It is applicable for Kola drill string where we have long distances and small deviatory inclinations.

First of all let us take a look at the drag forces for straight inclined wellbore section without pipe rotation. Pipe tension in the strait wellbore section is not contributing to the normal pipe force, and hence not affecting friction. Straight section becomes weight-dominated as only the normal weight constituent gives friction [3]. Top force of the pipe F_2 defined as follows:

$$F_2 = F_1 + \beta \Delta L w(\cos\alpha \pm \mu \sin\alpha) \quad (4.10)$$

Here ΔL - the length of segment of the pipe; F_1 – additional force caused by the weight of the pipe below considering section; w - unit pipe weight; α - wellbore inclination; μ - friction coefficient; "+" stays for lifting up and " –" stays for lowering down the pipe.

Torque for inclined wellbore section without axial motion defined as a normal weight component $\beta w \Delta L \sin\alpha$ multiplied by the radius of pipe tool joints r and coefficient of friction μ:

$$T = \mu r \beta w \Delta L \sin\alpha \tag{4.11}$$

Let take a look at drag force for curved wellbore section without pipe rotation. The normal contact force between string and hole is strongly depends on the axial pipe loading. This is therefore a tension-dominated process. The tension in the relatively short bend may be much larger than the weight of the pipe inside the bend segment. Here comes the assumption that the weight of the pipe is imponderable when the friction computed, but weight at the end of the bended pipe should be added. Moreover, the dogleg angle θ depends both on the wellbore inclination and the azimuth. The pipe will contact either the high side or the low side of the wellbore and its contact surface is given by the dogleg plane [3]. Equation for the axial force becomes as follows:

$$F_2 = F_1 e^{\pm\mu|\theta_2-\theta_1|} + \beta w \Delta L \left(\frac{\sin\alpha_2 - \sin\alpha_1}{\alpha_2-\alpha_1}\right) \tag{4.12}$$

Equation is true for build-up, drop-off, side-bends or combination of the sections. Here "+" as before stays for hoisting and "–" stays for lowering of the pipe. This equation very easy to use if it is written as follows:

$$F_2 = F_1 e^{\pm\mu|\theta_2-\theta_1|} + \beta w R \sin\alpha \tag{4.13}$$

Here $\Delta L = R \cdot \alpha$.

Torque for a curved wellbore section without axial motion defined as follows:

$$T = \mu r N = \mu r F_1 |\theta_2 - \theta_1| \tag{4.14}$$

Where θ_1- dog-leg angle corresponding to the lower end of the section and θ_2 - dog-leg angle corresponding to the upper end of the section.

Consequently friction for any wellbore shape can thus be computed by dividing the well into strait and curved elements. The forces (equations 4.10 and 4.12) and the torques (equations 4.11 and 4.13) summed up from the bottom to the top of the well consecutively. At the very bottom of the string tension and weight dominated friction is so small that can be neglected. $F_1 = 0$ is used as an end state [3].

The above formulas interpretation must be modified if the combined axial and rotation motions take place. The physical effect of combined motion is well known, when the surpassing speed of rotation reduces vertical drag forces. In the source [9] described how the frictional capacity unscrambled into the two directional compounds, axial motion and rotation. Assuming V_h - axial speed of motion and V_r - tangential speed of rotation of the pipe. These two components give resulting vector V. On the figure 12 shown the graphical interpretation of the components and the angle between two velocities [3].

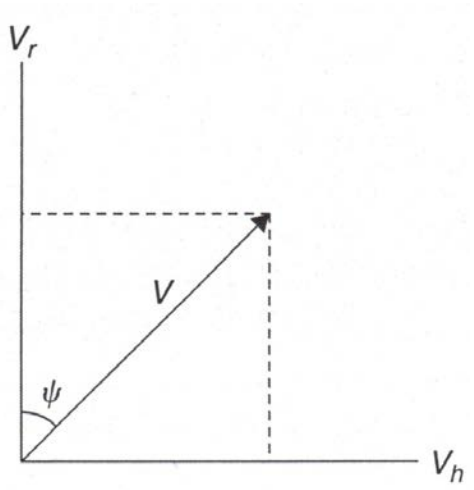

Fig. 12 Resultant speed components of axial and tangential motions.

The angle between the resultant and tangential velocities given as follows:

$$\psi = tan^{-1}\left(\frac{V_h}{V_r}\right) = tan^{-1}\left(\frac{60V_h(m/s)}{2\pi N_r(rpm)r(m)}\right) \quad (4.15)$$

Equations of the torque and drag for combined motion in the straight pipe section are:

$$F_2 = F_1 + \beta\Delta Lw\cos\alpha \pm \mu\beta\Delta Lw\sin\alpha\sin\psi \quad (4.16)$$

$$T = \mu r\beta w\Delta L\sin\alpha\cos\psi \quad (4.17)$$

Equations of the torque and drag for combined motion in the curved pipe section are:

$$F_2 = F_1 + F_1(e^{\pm\mu|\theta_2-\theta_1|} - 1)\sin\psi + \beta w\Delta L\left(\frac{\sin\alpha_2 - \sin\alpha_1}{\alpha_2-\alpha_1}\right) \quad (4.18)$$

$$T = \mu rN = \mu rF_1|\theta_2 - \theta_1|\cos\psi \quad (4.19)$$

During the drilling the well on Kola Peninsula the turbine motor of gear reduction type were used. This method of drilling does not imply any rotation of string during the drilling itself. But in the sours [2] given the amount of unique experimental field data, which shows that a certain rotation rate of two revolutions per minute may be allowed during tripping out of drill string. In addition it would be constructive to suggest the presence of top drive application initiating the rotation of drill string during the lifting operations complicated by the increased friction in the open borehole and stuck pipe risks. So we will review the modeling of the string including the rotation as a separate part.

4.2 Drill string for ultra-deep drilling

Reliable and proven work of drill string under the high loads and temperature in the deep boreholes becomes a matter of calculations and important engineering work. The weight parameters and arrangement of the drill string and its separate elements have an impact on mechanical and economical drilling indicators that diminish the choice of pipe material, their anticipated values of primary physical properties and safety factors.

In the following chapter we will look at the core elements of the pipe material study, describe the aluminum drill pipe used for drilling of SG-3 and see the connection between the proposed above calculation model of the string and drill pipe characteristics.

4.2.1 Concept of drill string material evaluation

The survey of the material used in the production of drilling pipe demanding implementation of concept such as specific strength study, which is pronounced by a ratio of yielding point to the specific weight of materials.

The degree to which the material can be deformed depends on value of an imposed to it load or stress. The principal of stress is therefore in the focus of material and metal mechanics. Nerveless, stress may not be measured directly [5]. Strain usually measured in laboratory and the stresses calculated later. The stress-strain relation is not a simple linear for the most of the material and its geometry can change dramatically (due to impurities of minerals, metals or chemical elements) improving the overall strength quality of the matter.

On the figure 13 shown a bar under tension with initial length l_0. After some axial load it elongates to the length l. The elongation will be $\Delta l = l_0 + l$.

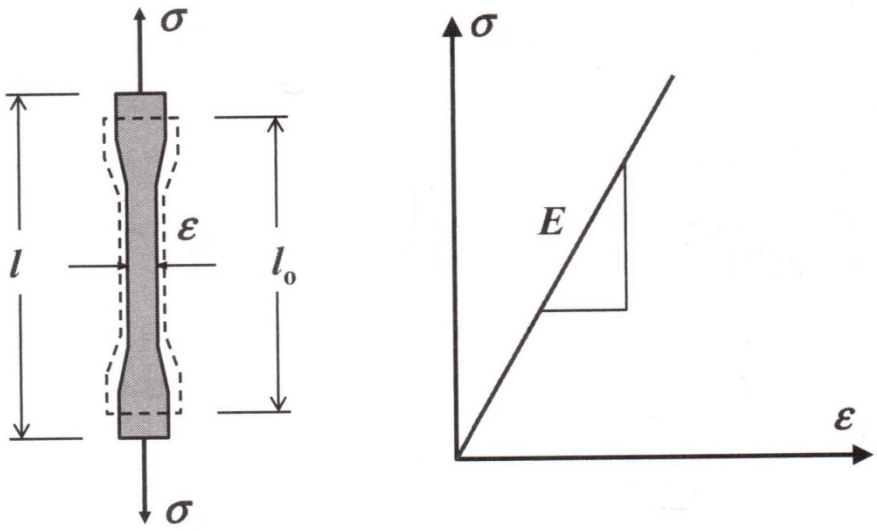

Fig. 13 Linear elastic deformation of the bar.

A linear part of relation between the stress σ and engineering strain ε that can be expressed by following formula known as Hooke's law:

$$\sigma = E\varepsilon \tag{4.20}$$

Where E - modulus of elasticity (Young's modulus). Stress and strain defined as follows:

$$\sigma = \frac{F}{A} \tag{4.21}$$

$$\varepsilon = \frac{\Delta l}{l_0} \tag{4.22}$$

The specific strength of a material may be expressed in terms of length and in its application to the drill string. It assigns the maximum length of a single-size drill string in the air. Wherein, the stresses in the suspended pipe body are equal to the yielding point of the material. In this case, the maximum length of the drill string is definite not only by the strength of pipe matter but

also by the distinction in specific weight of pipe and drilling mud [7]. Buoyancy aspects we had already reviewed in the previous section.

4.2.2 High strength aluminium drill pipes

At the Kola ultra-deep SG-3 well Aluminum Drilling Pipes (ADP) of different alloying elements were used. Variation in the selection of pipe types was dictated by the following main factors:

- acting loads;
- required durability of operations;
- temperature on the certain depth;
- allowable dimensions of the OD of the pipe.

The drill string was constructed of light alloying aluminum pipes with primary 147 mm OD and internal pipe end upset (Figure 14). It was provided four options of pipe's wall thicknesses: 11, 13, 15 and 17 mm.

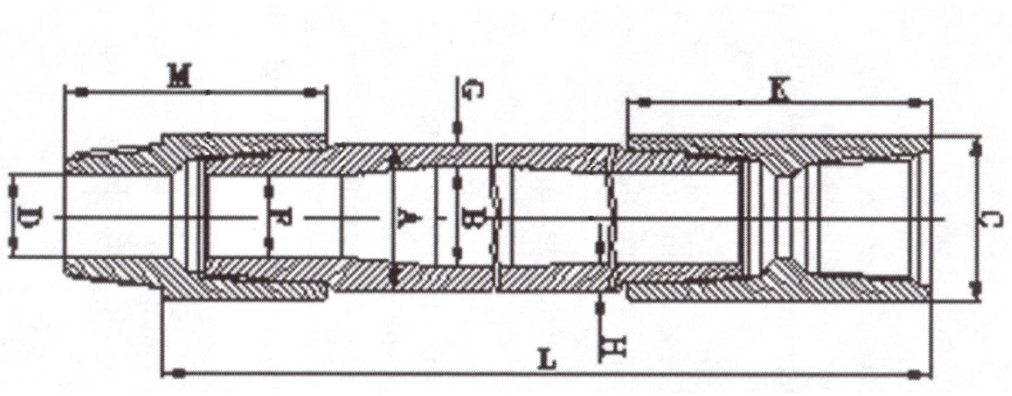

Fig. 14 ADP with internal upset ends [7].

This type of light alloying ADP with internal end upset and conical stabilizing ends called in Russian transcription LBTBK-147 (English translation as follows: LDPIC-147. Here L- light alloying, D – drilling, P – pipes, I – with internal end upset, C - with conical stabilizing ends, 147 - size OD in mm) and steel tool joints (ZLK-178) specially designed for drilling of deep and ultra deep well bores by turbine and rotary technique [2]. The connection between the tube and the joint consist of conical trapezoidal thread in combination with a smooth conical stabilizing surface and eliminates the cut of thread fatigue failure. This significantly increases the reliability and durability of light alloying ADP. The presence in the tube-joint compound of conical surfaces coupled with the tension and also internal abutment surfaces ensures high sealing integrity of the mentioned connection.

In the conjunction applied trapezoidal thread with the taper of 1:32, pitch of 5.08 and profile angle of 30 degrees. Use of such thread with conjunction in the inner diameter and only one side of profile allows it to support accurate landing of the thread in the screwed connection. Stabilizing belt also configured with the taper 1:32. That's why endurance limit of LBTBK pipes gradually higher than the limits of standard ADPs.

It is noteworthy that pipe assembling can be carried out both by hot and by could manner. During the hot assembling it should be taking technical measures to limit warming of the pipe in the contact with the steel lock until the certain value by internal cooling of the pipe. It made to save initial indices of mechanical properties for aluminum alloys. Table 3 represents the specification of ADP used for drilling of this super deep well [2, 7].

During the drilling of SG-3 well in the interval of 8000 m the light aluminum pipes of standard construction were used with light build tool joints type (ZL-172). At the greater depths were used advanced ADPs of LDPIC-147 type from the different allows (D16T, 1953T1 and AK4-1T1) with advanced steel joints (ZLK-178) using steel marks 40HN and 40HMIFA [2].

Table 3 Specification of aluminum drill pipes with internal pipe end upset.

Nominal pipe length, m:				
- **without tool joins**	12	12	12	12
- **with tool joints**	12,4	12,4	12,4	12,4
Wall thickness, mm:				
- **G**	11	13	15	17
- **H**	17	20	22	24
Pipe body cross-section, cm^2:	47,0	54,7	62,2	69,4
Nominal diameter of the pipe, mm:				
- **A**	147	147	147	147
- **B**	125	121	117	113
- **F**	113	113	113	113
Nominal diameter of the joints, mm:				
- **ID-joint D**	110	110	110	110
- **OD-joint C**	178	178	178	178
Box member length – K, mm:	350	350	350	350
Pin member length – M, mm:	350	350	350	350
Thread connections type:	5 ½¨ FH	5 ½¨ FH	5 ½¨ FH	5 ½¨ FH
Specific weight of the pipe, kg/m:				
- **without tool joints**	13,9	16,1	18,2	20,1
- **with tool joints**	18,8	21,0	23,1	25,0

Different allows application stipulated by the different environmental working condition of the pipes in the different intervals of the well. Main factors here were effective stresses and ambient temperature. Drag forces along the drill-string and others ADP elements, wear etcetera were taken into account. In this case the main engineering task became to develop recommendations on the choice of materials, design criteria of ADPs and optimal assemblage in extremely harsh environment.

4.2.3 High strength steel drill pipes.

On the very lower and very upper parts of the drill-string high strength steel drilling pipes (SDP) has been used. Steel drill-pipes called in Russian transcription TBVK-140 (English translation as follows: DPIC-140. Here D – drilling, P – pipes, I – with internal end upset, C - with conical stabilizing ends, 140 - size OD in mm) with internal end upsets and conical stabilizing belts and tool joints of ZSK-178 type designed for drilling deep and ultra-deep boreholes in the hard and complicated conditions by rotary and turbine method. Table 4 shows main parameters of the SDP used for drilling on Kola rig [2].

Table 4 Specification of steel drill pipes with internal end upset.

Thickness of the pipe wall, mm	10	11	12	13.5
Internal diameter of internal end upset, mm	100	100	100	98
Length of the end upset, mm	155	155	160	160

The connection between the tube and the tool joint consist of conical trapezoidal thread in combination with a smooth conical stabilizing surface and eliminates the cut of thread fatigue failure. This significantly increases the reliability and durability of SDP. The presence in the tube-lock compound of conical surfaces coupled with the tension and also internal abutment surfaces ensures high sealing integrity of the connection. Table 5 shows main parameters of tool joint ZSK-178 type used for SDP.

Table 5 Main parameters of ZSK-178 tool joints for steel drilling pipe.

Outer diameter of joint, mm	178
Inner diameter of joint, mm	101
Length of assembled joint, mm	573
Thread connection type	5 ½¨ FH
Weight of tool joint, kg	61

Tool joint attaching to the steel pipe carried out only by hot manner. During the joint assembling pipe is heated up to 400-450ºC. In the conjunction applied specially developed trapezoidal thread with the taper of 1:32, pitch of 5.08 and profile angle of 30 degrees, same as for ADP. Use of such thread with conjunction in the inner diameter and only one side of profile allows it to support accurate landing of the thread in the screwed connection. Stabilizing belt also configured with the taper 1:32. Endurance limit of TBVK pipes gradually higher than the limits of standard SDPs.

For manufacturing of steel pipes was used a steel of 30HGSNM mark, and for tool joints was used the steel of 40HN and 40HMIFA marks. Mechanical properties of the steel types used for pipe body and for toll joint both in SDP and ADP listed below in the table 6 [2].

Table 6 Mechanical properties of the steel used for manufacturing SDP pipe body and ADP tool joints.

Physical property	**SDP pipe body 30HGSNM**	**ADP tool joints 40HN**	**ADP tool joints 40HMIFA**
Yield strength, MPa	900	750	800
Tensile strength, MPa	1000	900	900
Hardness, HBr	285-370	285-341	285-363
Elongation, %	12	10	14
Reduction of area, %	40	45	50

4.3 Aluminum alloys selection for ultra-deep drilling.

The weight characteristics of the pipe body and it weight reduction during the mud circulation fated the value of tension in various cross-section of the string and affect it operational endurance. During the ultra-deep drilling operations, the lower part of the string and BHA is usually exposed for the long-term influence of the high temperature zone that degenerates the strength properties of drilling tubes metal and therefore restricts penetration depth. That fact predetermined the necessity of selection of thermo-resistant aluminum alloys to be used in the lower part of the drill string and to evolve sustainable method of their analysis and operation.

Based on the previous studies for the specified conditions have been specially developed following alloys:

- D16T – alloy of Al-Cu-Mg well mastered by the industry. It hardened by heat treatment and has average strength characteristics. Alloy has corrosion resistance and thermal stability up till 160˚C. Pipes of this type characterized by the highest plasticity if compared to others alloys. Estimated descent depth of this type pipes in the region of drilling SG-3 is 9500 m.
- 1953T1 – high-strength alloy of Al-Z-Mg-Cu specially developed for manufacturing of drilling pipes and well mastered by the industry [10]. This type of alloy hardened by heat treatment and has average corrosion resistance. It has thermal stability up till 120˚C and allowable operational depth of the pipe is up to 6000 m.
- AK4-1T1 – alloy of Al-Cu-Mg-Fe-Ni widely used for press-manufacturing industry. It hardened by heat treatment and has average strength characteristics and corrosion

resistivity. Alloy has improved thermal stability up till 240˚C. Recommended allowable operational depth of this type pipes is up to 13000 m.

Mentioned above alloys meet not only the requirements of drilling operation, but they also are easy to produce and allowed organizing of mass production of the pipes with variable diameter along the length. Physical and mechanical characteristics of the aluminum alloys under normal temperature conditions footnoted to the table 7 [7].

Table 7 Properties of aluminum alloys for ADP under normal conditions.

Characteristic	D16T	1953T1	AK4-1T1
Yield strength, MPa	330	490	350
Tensile strength, MPa	450	530	410
Hardness, HBr	120	125	130
Elongation, %	11	8	12
Reduction of area, %	20	15	26
Specific gravity, N/m^3	28000	28000	28000
Modulus of elasticity, MPa	72000	70000	73000
Shear modulus, MPa	26000	27500	27500
Poisson's ratio	0.33	0.31	0.31
Thermal expansion coefficient, $1/C^0 \cdot 10^{-6}$	22.5	23.8	23.8
Max allowable operating temperature, C^0	160	120	240

According to experimental study and long-term operation experience there are three temperature zones for ADP operations that can be distinguished. The first zone characterized by mechanically stable ADP and it design strength factor should be equal to the material yielding point at 20^{o}C. It is a commonly accepted prevalent approach of designing drill-string for most of the oil and gas wells.

Within the second zone, operational temperature is growing and the mechanical strength of pipe metal is visibly reduced and operation time became an important factor. The yielding point of material basically determined after 500 hours of exposure to the given temperature. This is used as a main design parameter. A period of 500 hours is selected as a worst case scenario of long-term exposure during the drilling problems occurring and elimination [7].

In case if ADP reaches the location, where the temperature exceeded the certain critical level, the plastic deformation occurs under multiple loads exposure. It results in structural changes and can lead to destruction of the pipe under gradually lower loads than those assumed in calculations at the standard conditions. Prolonged strength limit of material becoming a dominative design parameter of ADP in this temperature zones. In the table 8 shown two design criteria that can be applied for three different type of aluminum alloys depending on temperature regime [7].

Table 8 Design criteria of ADP under various temperature of operation.

Alloy type	Design criteria	
	Yield strength after 500 hours at the operational temperature	**Prolonged strength limit at the operational temperature based on 500 hours exposure**
D16T	120-145^{o}C	145-200^{o}C
AK4-T1	140-160^{o}C	160-200^{o}C
1953T1	90-115^{o}C	Not applicable

Earlier we had described the type of thread connections of the aluminum drill pipes it construction and particular features. So, one of the most important operational parameter of drill-string is the endurance and durability of its thread connection. Lab testing provides the

experimental data on durability and endurance limit of thread connections that usually used for designing drill-string. Same method used for selection of pipe connection type, threads design and there stress deformation state. On table 9 shown experimental results concerning limits of endurance of various elements of 147 mm OD ADPs based on 10^7 oppositely changing loads with frequency of 650 cycles per minute [7].

Table 9 ADP fatigue strength for 147 mm OD pipe with steel tool joints (based on 10^7 cycles with frequency 650 c/min).

Testing element of ADP	Type of alloy	Fatigue strength, MPa
Pipe body	D16T	110
ZL type of tool joint to pipe connection with triangle thread profile	D16T	47
	1953T1	40
ZLK type of tool joint to pipe connection with acme thread profile and tapered belt behind the thread	D16T	64
	AK4-1T1	70

Here, in description of pipes used in drilling we got several tables with data on the physical properties of metals used in constructing of drilling pipes. Comparing strength of this metals combining drill-string we have to choose the weakest point in the string and apply to the properties of metal having lower strength in the pipe assemble. For both the ADP and SDP it will be pipe body properties. Tool joints threads connections of SDP made from the lower grade steel and have worst strength characteristics, but it construction and body cross-sectional area making this element more reliable compares to pipe itself. For calculation of allowable pull out loads dominative for as becomes not fatigue strength and not a tensile strength, but yielding strength, which displays the ability of the material to withstand continuous loads elastically and not destroying internal structure of the metal.

A number of the mentioned above parameters will be applied in the drill pipe optimization section, where we try to compose the drill string based on described criteria and experience borrowed from the history of drilling SG-3.

5 Drill string optimization

In the next part we will try to offer the optimum design of the drill string. Further, applying to the above mentioned theory we will try to consider different cases and scenarios of drilling starting with the ideal scenario of perfectly vertical drilling. Later we will gradually complicate the task maximally narrowing to reality of drilling ultra-deep wells. Finely we will look at the complex shaped of well and evaluate reliability of dual aluminum-steel drill-string proposed for Kola SG-3 project.

It should be noted that optimization of the drilling string is a complex dynamically changing tack, which depends on many actual factors (such as wellbore stability, mud density, deviation of well path, friction and others) speed, and current methods of collecting information. It cannot be solved only by assessment and planning human work. In the resent days complex computing tools and integration online predicting models used on a daily basis, while conducting drilling operations. But we can reduce the risk of occurring problems by study of best world practical experience and working out a technical intuition. This is exactly what we will do in the next section.

5.1 Proposed drill string assemblage.

Taking into account all complex of information relating to the tensile properties of the alloys, expected loads on drill string and temperature conditions in borehole let us to suggest following assemblage of drill string for drilling 12 262 m deep well described in the table 10. Here we can see combination of different alloys distributed on the different depth according to the zonal conditions and design factors described earlier.

Wall thicknesses and pipe body cross-sections taken from the specification described in earlier chapters. Temperature at the location in the bore hole calculated out of the information about maximum recorded temperatures at the achieved depth, which is around 220^{o}C. Assuming average temperature gradient through the all strata and temperature at the surface at the moment of record around +15^{o}C (assuming summer time at the Kola peninsula location, when temperature in the borehole could reach the maximum levels), we can assume the average gradient of (220-15)/12,26 = 16,7 ^{o}C/km.

For us is not important to review the deviation from the average temperature gradient. In the condition when the mud is pumped in accurate temperature cannot be determined and is not essential for us. But it is very important to take into account temperature degradation of the drill-string based on worst case scenario and include that factor in our calculation of allowable tensile load.

Table 10 Drill-string assemblage for Kola SG-3.

Number of the section	**Drill string type**	**OD, mm**	**Wall thickness, mm**	**Type of alloy**	**Pipe body cross-section, cm^2**	**Temperature at the depth, ^{o}C**
1	BHA	-	-	-	-	220
2	SDP	140	10	30XGSNM	40.8	188
3	ADP	147	11	AK4-1T1	47.0	169
4	ADP	147	13	AK4-1T1	54.7	145
5	ADP	147	15	D16T	62.2	122
6	ADP	147	11	1953T1	47.0	102
7	ADP	147	13	1953T1	54.7	82
8	ADP	147	15	1953T1	62.2	65
9	ADP	147	17	1953T1	69,4	18
10	SDP	140	11	30HGSNM	44.6	16

Table 10 - Continuation. Drill-string assemblage for Kola SG-3.

Number of the section	**Section length, m**	**Cumulative length, m**	**Specific weight of the pipe, kg/m**	**Section weight in the mud, kN**	**Cumulative weight in the mud, kN**	**Allowable tensile load at 20°C, kN**	**Allowable tensile load at the actual temperature in the borehole, kN**
1	40	40	150	50	50	-	-
2	150	190	34.4	43	93	3672	3488
3	2800	2990	18.8	305	398	1645	1316
4	1000	3990	21.0	122	520	1914	1531
5	1200	5190	23.1	160	680	2053	1745
6	1200	6390	18.8	131	811	2303	1958
7	1400	7790	21.0	170	981	2680	2278
8	1450	9240	23.1	194	1175	3048	2591
9	1100	10340	25.0	159	1334	3400	2890
10	1920	12260	40.5	648	1983	4014	3813

Section weight in the mud calculated as follows. Out of the physical properties of metals we know the densities of steel equal to 7,8 g/cm^3 and aluminum equal to 2,8 g/cm^3. Assuming densities of drilling mud at the depth of 12 km taken from the primary source [2] equal to 1,15 g/cm^3, corresponding buoyancy factors becomes 0,85 for steel pipe and 0,59 for aluminum sections. By multiplication of specific weight of the pipe by length of the section and buoyancy factor, we estimating section weight in the mud.

For calculation of allowable tensile load of drill-string we are taking into account yield strength of the material of the weakest element on the assembled pipe. For both ADP and SDP it will be pipe body itself with the following yield strength characteristics of the materials:

	30HGSNM	AK4-1T1	D16T	1953T1
Yield strength, MPa	900	350	330	490

Allowable tensile load at normal conditions (20°C) calculated by formula:

$$F = \sigma_y \cdot A \cdot 10^{-1} \quad (5.1)$$

Where σ_y – yield strength of the material in MPa; A - pipe body cross-section in cm^2; 10^{-1} - unit conversion factors for result in kN.

Then, to calculate actual allowable limit, we have to include temperature degradation factor. On the reviewed depth and temperature conditions assuming following weakening of the metals (based on material degradation graph from appendix):

	30HGSNM	AK4-1T1	D16T	1953T1
Yield strength degradation, %	5	20	15	15

Now allowable tensile load at the resent temperature condition in borehole can be calculated by reducing yield strength on the value of material degradation. By these results the first part of calculations can be accomplished. Further we have to take a look at the different drilling scenarios capable to generate additional frictional forces on the drill-string and influence on the general physical picture of proposed assemblage. We will review a factor different well geometry that can create drag forces in the borehole:

5.2 Ideal vertically drilled well.

Initially SG-3 has been designed to be a purely vertical well. Let as first of all review unrealistic scenario of absolutely vertical 12 km long well. As we know from the theory there are no frictional forces in purely vertical well between drill-string and borehole wall and all load to the string supposed to be formed by the weight components. Then results will be equal to calculated cumulative weight in the mud presented in the table above.

There is one factor that can affect pull out force on the hook and create additional component to the weight. It is frictional forces or with another word to say, break-out-forces of mud itself. This significant at the initial moment force dramatically falling down almost to the zero during the first seconds of initiated motion and can be palpable on the huge depths. Mud factor depends on the chemical composition of the mud itself and its physical viscosity properties. The effect of drug forces will depend also on outer diameter of drill-string and its tool-joints at any particular depth.

Considering this peculiarity during the extended drilling pauses on big depths can be recommend to rotate the drill-string prior to pulling it out. This is especially critical for the wells, where drilling mode provided by the turbine motor and additional rotation top drive likely would be envisaged. However, for our calculation we will assume mud factor as not a very sensitive and neglect it with the mentioned above assumptions. In a table 11 provided pull-out load calculation and safety margins forming in the proposed drill-string assemblage for the ideally vertical well.

Table 11 Pull-out load results of ideally vertical well.

Number of the section	Cumulative weight in the mud, kN	Pull-out load, kN	Allowed pull-out (tensile) load, kN	Safety margin, kN	Safety margin, %
1	50	50	-	-	-
2	93	93	3488	3395	97
3	398	398	1316	918	70
4	520	520	1531	1011	66
5	680	680	1745	1065	61
6	811	811	1958	1147	59
7	981	981	2278	1297	57
8	1175	1175	2591	1416	55
9	1334	1334	2890	1556	54
10	1983	1983	3813	1831	48

From the table is seen interesting singularity. Safety margin presented in percents interpreting the reliability of drill-string. It is clearly observed the falling trend of reliability from the bottom of the well to the top in the vertical borehole, where drag forces not yet implemented.

5.3 Three-dimensional well geometry.

During designing SG-3 drill-string it would be wrong to assume perfect well path control and relay on the prediction of ideal vertical drilling of 13 km long well. Contrariwise, engineering approach basically involves worst case scenario issue. Following this logic we also should make a number of reasonable assumptions concerning drilling path and corresponded drag forces.

Based on foregoing we can include two logical assumptions (factors) in the process of predicting of well path for 13 km primary vertical well:

- unperfected vertical drilling with deviation of max 10^{o} per 1 km (spiral shape of well) from the depth of 2000 m, where well path control for the technology of 20^{th} century becoming unreliable (most probable worst scenario);

- side track due to disrupted well bore stability on the depth, where it is most likely possible (out of the analysis in the chapter 3.3 devoted to the wellbore stability of the resent thesis).

Out of the conducted analysis during the drilling at a depth of 5700 m, 6700 m as well as deeper than 10000 m complications may occur. So we can assume side track scenario on the one of this depth, as well as several of them. Returning to the calliper log data from the figure c we can see, that stability problems stars to appear at the depth of around 5000 m with some shocks at the level of 6000 m. Later at 7000 m and deeper stability gradually decreases again. From the drilling history of SG-3 we know that sidetracking took place at 7000 m. Let assume this level also for our drill-string stress analysis with dog-leg-severity of 15^o per 1 km.

Concluding all mentioned above findings let us to propose following well geometry (fig. 15) for the further drug force calculations.

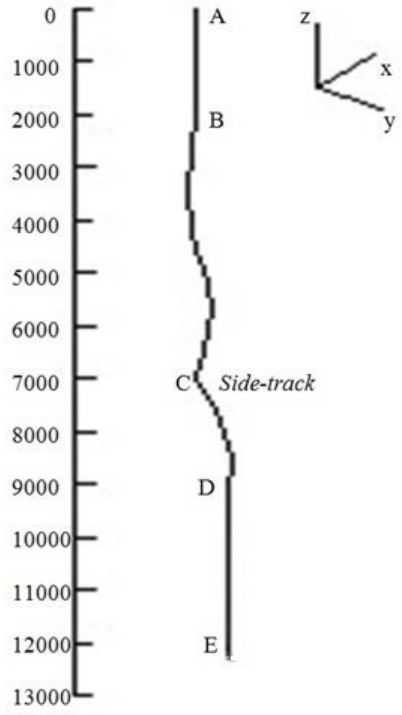

Fig. 15 Sketch of proposed well geometry.

Here we have purely vertical section A-B from 0 to 2000 m depth; B-C spirally shaped section with dog-leg-severity of 10^o per km on the depth from 2000 to 7000 m consisting of two parts (one spirally build-up part with length of 2500m and one spirally drop-off section of length 2500 m) ; C-D combined equal build-up and drop-off sections with dog-leg severity of 15^o per km on the depth from 7000 to 8700 m (build-up from 7000 to 7850 m and drop-off from 7850 to 8700 m); D-E vertical section on the depth from 8700 to 12260 m.

As we know from the theory, the static hook load is equal to the buoyed pipe weight multiplied by the projected vertical height of the well, regardless of wellbore orientation. Horizontal displacement of all of these sections will be relatively small and due to insufficient information about difference between TMD and TVD we will use value of projected length equal to the measured length. It will not affect the calculation of forces in a decreasing manner and satisfy to the worst case principal.

Let first calculate static, hoisting and lowering weight starting from the bottom. Static weight we calculate based on information presented in the table 10 using of value of correspondent section weight. Here is example of static load calculation for position D:

D: ΔL=12260-8700=3560m

Section number	Length, m	Static load in the mud, kN		Total length of section 4 is 1000 m. We have only 570 m of section 4. Proportion: $\frac{1000m}{100\%} = \frac{570m}{x}$; x= 57% Weight of 1000 m of section 4 is 122 kN; weight of 570 m of section 4 is: 122kN·0.57=70 kN
1	40	50		
2	150	43		
3	2800	305		
4	570	70	→	
Sum:	3560	468		

All results of ongoing calculation we tabulate in the table 12.

Table 12 Drug forces of proposed drill-string.

Position o the drill-string	Static weight of section in the mud, kN	Hoisting force, kN	Lowering force, kN
E	0	0	0
D	50+43+305+70=468	468	468
C	468+(52+160+8)/2=578	468·1.045+109=598.1	468·0.956+109=556.4
	578+(52+160+8)/2=688 (TVD assumed = TMD)	598.1·1.045+109=734	556.4·0.956+109=640.9
B	688+(123+170+194+148)/2=1006	734·1.09+307.8=1107.9	640.9·0.916+307.8=894.9
	1006+(123+170+194+148)/2=1324	1107.9·1.09+307.8=1515.4	894.9·0.916+307.8=1127.5
A	1324+11+648=1983	1515.4+11+648=2174.4	1127.5+11+648=1786.5

Calculating dog-leg angle for section C-D consisting of two equally composed - one build-up and one drop-off sections (850 m each): DL = DLS · ΔL = 15 deg/km · 0.85 km = 12.75°; $\theta(rad) = 12.75° \cdot \frac{\pi}{180} = 0{,}222\ rad$

Assuming friction coefficient equal to $\mu = 0{,}2$ computing frictional factor:

$$e^{\pm\mu(DL\frac{\pi}{180})} = e^{\pm 0.2(12.75\frac{3.14}{180})} = \begin{cases} 1.045\ for\ hoisting \\ 0.956\ for\ lowering \end{cases}$$

Average buoyed unit weight of the pipe (52+160+8)/1700 = 0.129 kN/m

Using formula 4.12 to calculate drag forces:

$$F_{h1} = 468 \cdot 1.045 + 0.129 \cdot 850 \cdot \frac{\sin 12.75}{0.222} = 489.1 + 109 = 598.1\ kN$$

$$F_{l1} = 468 \cdot 0.956 + 0.129 \cdot 850 \cdot \frac{\sin 12.75}{0.222} = 447.4 + 109 = 556.4\ kN$$

$$F_{h2} = 598.1 \cdot 1.045 + 0.129 \cdot 850 \cdot \frac{\sin 12.75}{0.222} = 625 + 109 = 734\ kN$$

$$F_{l2} = 556.4 \cdot 0.956 + 0.129 \cdot 850 \cdot \frac{\sin 12.75}{0.222} = 531.9 + 109 = 640.9\ kN$$

Calculating dog-leg angle for section B-C consisting of two equally composed - one build-up and one drop-off sections (2500 m each): DL = DLS · ΔL = 10 deg/km · 2.5 km = 25°; $\theta(rad) = 25° \cdot \frac{\pi}{180} = 0{,}436\ rad$

Computing frictional factor:

$$e^{\pm\mu(DL\frac{\pi}{180})} = e^{\pm 0.2(25\frac{3.14}{180})} = \begin{cases} 1.09\ for\ hoisting \\ 0.916\ for\ lowering \end{cases}$$

Average buoyed unit weight of the pipe (123+170+194+148) /5000 = 0.127 kN/m
Using formula 4.12 to calculate drag forces:

$$F_{h1} = 734 \cdot 1.09 + 0.127 \cdot 2500 \cdot \frac{\sin 25}{0.436} = 800.1 + 307.8 = 1107.9\ kN$$

$$F_{l1} = 640.9 \cdot 0.916 + 0.127 \cdot 2500 \cdot \frac{\sin 25}{0.436} = 587.1 + 307.8 = 894.9\ kN$$

$$F_{h2} = 1107.9 \cdot 1.09 + 0.127 \cdot 2500 \cdot \frac{\sin 25}{0.436} = 1207.6 + 307.8 = 1515.4\ kN$$

$$F_{l2} = 894.9 \cdot 0.916 + 0.127 \cdot 2500 \cdot \frac{\sin 25}{0.436} = 819.7 + 307.8 = 1127.5\ kN$$

The torque we calculating by formula 4.14. Results presented in the table 13.

Table 13 Torque calculation of proposed drill-string geometry.

Position of the drill-string	**Torque calculation, kN**
E	0
D	0
C	0.2·0.147/2·468·0.222=1.53 1.53+0.2·0.147/2·578·0.222=1.53+1.89=3.42
B	3.42+0.2·0.147/2·688·0.436=3.42+4.41=7.83 7.83+0.2·0.147/2·1006·0.436=7.83+6.45=14.28
A	14.28

Obtained results can be presented as a graph. On figure 16 shown axial loads and on figure 17 presented calculated torque.

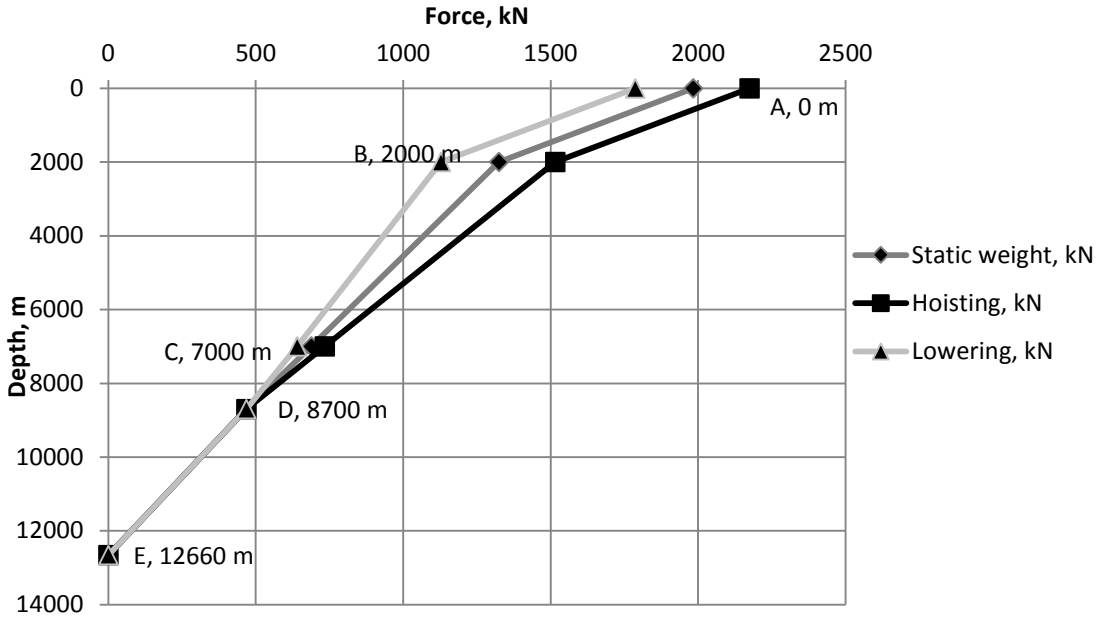

Fig. 16 Plot of calculated axial loads on drill string.

Correlating the data from the plot according to the section length of proposed drill string assemblage we obtain following results of drag forces combined in the table 14. Mathematically we call it linear interpolation.

Table 14 Drag forces on sections of drill string during tripping operations.

Number of the section	Cumulative length from the bottom, m	Actual depth, m	Static cumulative load, m	Cumulative load during the hoisting, kN	Cumulative load during the lowering, kN
1	40	12220	50	50	50
2	190	12070	93	93	93
3	2990	9270	398	398	398
4	3990	8270	535	550	520
5	5190	7070	700	740	650
6	6390	5870	850	920	760
7	7790	4470	1000	1140	880
8	9240	3020	1200	1360	1030
9	10340	1920	1370	1550	1060
10	12260	0	1983	2174	1787

Computing of combined rotation and tripping motion will not be conducted because it is not sensitively affect loads in our case due to low rotation speed of the string. For the Kola ultra deep drill string design, where turbine motor used for drilling and the rotation of drill string expected with the speed not higher than 2 RPM. It will create some external stresses in the string body but not sensitively affect the friction force derivative during tripping operation.

For real case of string design combined stress of tension and rotation should be compulsory computed. Following formula can be used:

$$\sigma_c = \sqrt{\sigma^2 + A\tau^2} \leq \sigma_l \qquad (5.2)$$

Where σ_c - combined load; σ- tension load; τ- rotation load; A – anisotropy coefficient of the pipe material; σ_l- strength limit.

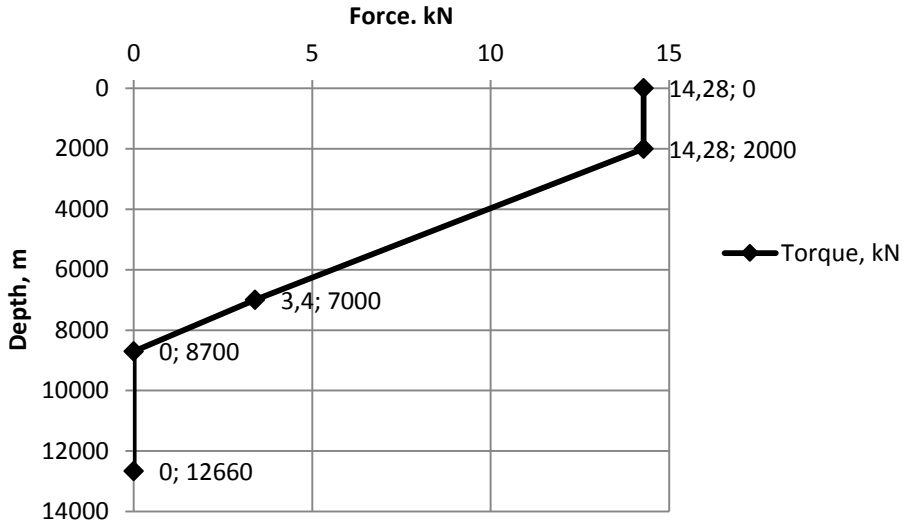

Fig. 17 Plot of calculated torque on drill string.

The figures above show how the bends in the wellbore affect friction. We can see that for the proposed well geometry drag forces on the hook increases for about 200 kN due to friction in the

bend. Therefore additional margin always should be included in the drill string design, which will take into account possible distortion in a planed wellbore geometry. For the Kola well safety coefficient was assumed of 1,3. Proposed above example alloys us to make conclusion about the size of the additional frictional values. No less useful will be to look at the actual field data from the Kola rig and compare it with the calculated above.

5.4 Dynamic of drug forces along the string according to the field data.

Operational condition of drill string in the ultra-deep wells in the solid impermeable crystalline rocks has their own characteristics. Among them: large depth of the well; significant amount of tripping works; large depths of outrunning open hole; complex geometry of the well; high abrasiveness and cavity of borehole with elliptical cross section; absence of filter cake on the borehole wall; absence of differential pressure effects.

Mentioned characteristics of interaction process between the drill string borehole wall and drilling mud causing increase of frictional forces. Under such forces we understand a combination of factors leading to excessive increase of hook load and in the different cross sections of drill string during the hoisting as well as increase in torque during the rotation of the drill string. Therefore resistance forces depends on physical and chemical properties of rock type and drill mud composition as well as geometry of well bore and form of cross section and length of open hole. Friction also depends on radial size and material of drill string.

Field experience of drilling SG-3 from the source [2] allows us to review the actually messaged loads and find some correspondence with the theoretically described model. Dynamic of drug forces change during the tripping up of drill string with increasing depth summarized in the table 15 and shown on figure 18. The speed of tripping was 1 m/sec.

Table 15 SG-3 field data of loads dynamic along the drill string.

Length of the drill string,	**Measured hook load, kN**	**Cumulative weight of the drill string, kN**	**Drag forces, kN**	**Total hoisting load, kN**
2000	480	270	80	350
2434	550	310	120	430
2798	600	370	110	480
3163	660	420	130	550
3528	710	470	130	600
3902	790	510	180	690
4277	850	560	190	750
4654	910	600	220	820
5027	990	650	260	910
5400	1050	690	280	970
5772	1120	740	310	1050
6145	1240	780	400	1180
6514	1300	830	420	1250
6889	1400	880	480	1360
7258	1500	930	540	1470
7633	1620	990	610	1600
8006	1750	1040	700	1740
8378	1900	1100	800	1900
8749	2040	1160	900	2060
9121	2220	1270	980	2250
9495	2500	1390	1170	2560
9866	2600	1510	1250	2750
10000	2680	1550	1120	2670

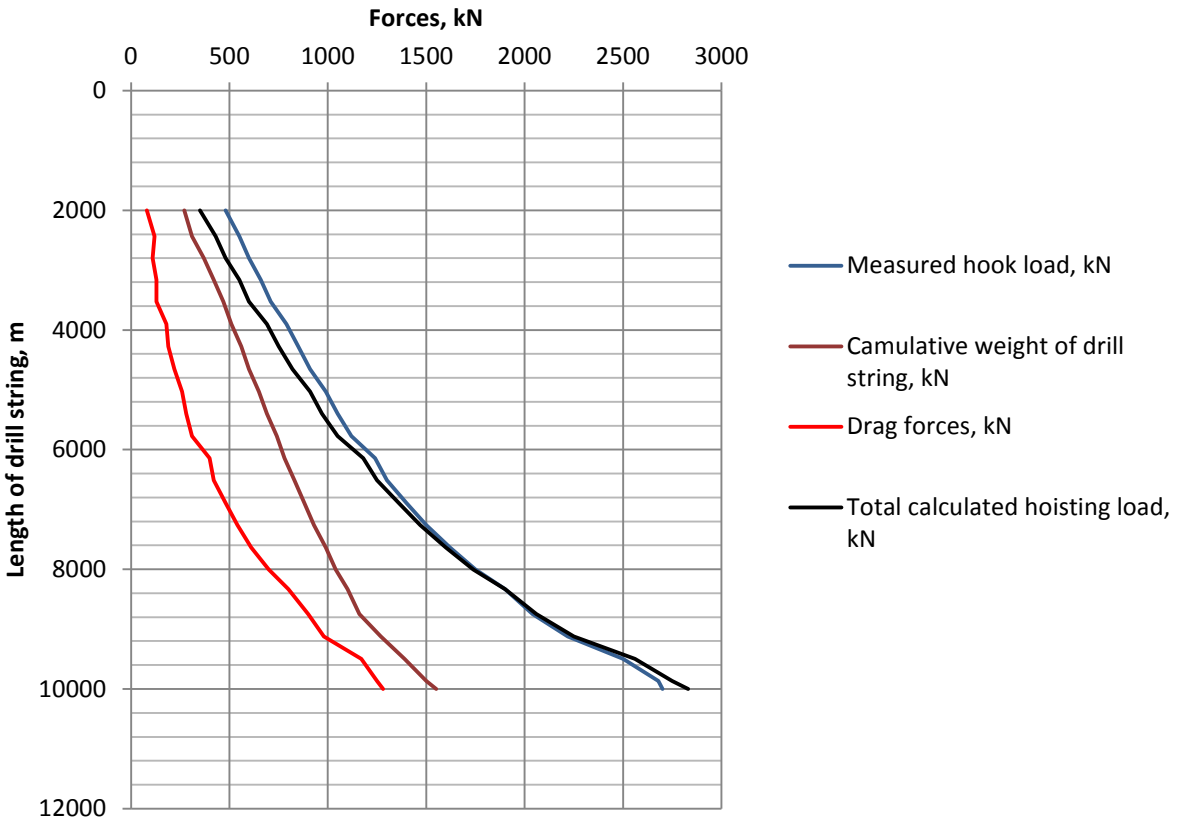

Fig. 18 Dynamic of drug forces change during the hoisting of drill string.

As it seen from the plot alteration of frictional forces with the depth has power law dependence (parabolic form of the figure). What is more dependence in the upper sections of the well (up to 7000 m) is closed to the linear with progressive growth with the depth. Maximum increase in the drug forces observed in 1 km zone of bit location. That indicates correspondence with existing geometrical friction model and shows that real geometry were similar to proposed by us in terms of drag forces. Smooth shape of the plots justified by huge volume of data involved.

Dynamic of torque change with increasing depth during the rotation of drill string with speed 2 rotation per minute (RPM) summarized in the table 16 and shown on figure 19.

Table 16 Dynamic of torque with increasing depth based on SG-3 field data.

Length of the drill string, m	**Measured torque, kN**
3011	0.5
4060	3.1
5010	6
6026	10.5
7030	13
8031	17
8920	21.3
10035	27.3
10213	27.4

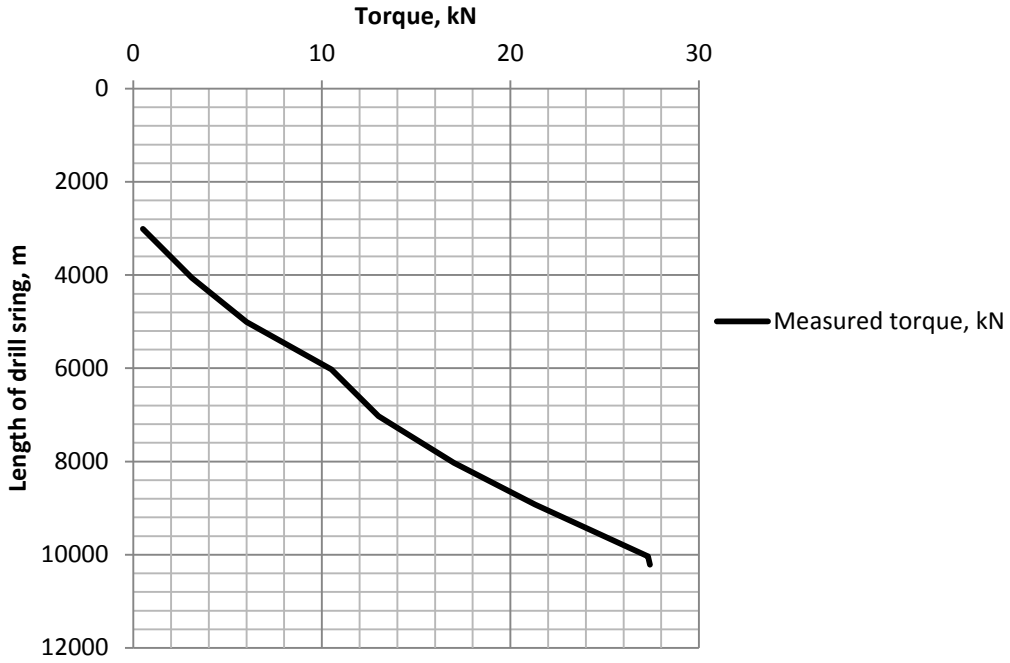

Fig. 19 Dynamic of torque change based on field data of SG-3.

Analyzing the change of frictional forces with increasing depth during the drilling of SG-3 it was made several conclusions.

During the deepening of the well together with the growth of total drill string contact length with borehole wall the value of derivative of frictional force in the upper sections decreases. It can be explanted by adjustment of borehole walls and consequently that leads to reducing of the influence of cross-sectional shape. Basically the shape of borehole wall and radial sizes of drill string sensitively affecting frictional loads. With increasing tripping speed in the borehole with elliptic cross section drag forces also grows.

Friction of drill string and borehole wall in case of SG-3 can be attributed to the maximum possible. That was confirmed by laboratory experiments where dependence of frictional coefficient and the contact pressure was studied. Significant effect on resistant forces had also the amount of crashed rock material in the borehole annulus.

5.5 Collation of modelled and field loads data.

In the following chapter let us compare modelled loads of proposed drill-string with the real field data of SG-3 project. It may help to review all complexity of drill string loads accumulation and its deviation from the pre-designed. Based on correlation with the field data it possible to assume a number of additional factors affecting load formation and use those assumptions together with certain safety margins in the next work of planning ultra-deep well. This is a core element of the optimization analysis reinforced by the unique experience of drilled well.

In the table 17 gathered all key data regarding the loads in the modelled and real field cases. Tabulated data can be interpreted both ways, by plotting the tensile loadings along the drill string (presented on figure 20) and by plotting the loads against the drilled depth (presented on figure 21). In first case it is convenient to look at the distribution of the loads along the lowered drill-string from the bottom to the top. In the second case the graph represents weight on the hook depending on the length of lowered drill-string and it is becomes comfortable to analyse achievable depth and correlate it this geological and geophysical conditions.

Table 17 Modelled and field case loads of optimised drill string.

Number of the section	Cumulative length from the bottom, m	Actual depth, m	Modelled static load, kN	Field static load, kN
1	40	12220	50	-
2	190	12070	93	-
3	2990	9270	398	396
4	3990	8270	535	521
5	5190	7070	700	668
6	6390	5870	850	813
7	7790	4470	1000	1011
8	9240	3020	1200	1308
9	10340	1920	1370	1652
10	12260	0	1983	≈2500 (interpolated)

Table 17 - Continuation. Modelled and field case loads of optimised drill string.

Number of the section	Modelled hoisting load, kN	Field measured hoisting hook load, kN	Calculated strength of drill string, kN	Safety margin according to the modelled hoisting load, kN;%	Safety margin according to the field data, kN;%
1	50	-	-	-	-
2	93	-	-	-	-
3	398	632	1316	918; 70%	684; 52%
4	550	804	1531	981; 64%	727; 47%
5	740	1016	1745	1005; 58%	729; 42%
6	920	1280	1958	1038; 53%	678; 35%
7	1140	1675	2278	1138; 50%	603; 26%
8	1360	2332	2591	1231; 48%	259; 10%
9	1550	2883	2890	1340; 46%	7; 0.2%
10	2174	≈3780 (interpolated)	3813	1639; 43%	33; 0.9%

Analysing gained results we can make several conclusions. Based on figure 21 reliable drilling occurred on the depth before 10 km where safety strength margin was above 10%. It says that contortion of the well geometry was unexpectedly high, what leads to occurrence of excessive stresses on the depths. Growth of loads here possibly was expected more linear and less intensive. This situation results in the coincidence of field hoisting load line and strength limit line on the figure 21.

One more evidence of excessive frictional loads is a high spread between field static load and field hoisting load. Compared with the modelled loads this spread is gradually higher. It means that together with more complex geometry were a number of others additional factors affecting the frictional force increase. We had already mentioned them earlier, but most critical after control of borehole trajectory become well bore stability, mud properties and cleaning capacity of the hydraulic system.

Issue of well bore stability returns us to the chapter 3.3.3 of the resent thesis where breath evaluation was conducted using unconventional approach. Looking at the figures 7 and 8 and combining with the data presented on the figure 21 very interesting observation coming up. Calliper log data on figure 8 indicating intensive destruction of the borehole wall starting from the 7500 m and on the figure 21 we can see observable change in inclination of field hoisting load approximately from the same depth. Stability limit for amphibolites formation on figure 7 crossing the line of maximal tangential stresses in the borehole wall exactly at the depth of 10000 m, where we have close junction of field hoisting and strength limit lines on figure 21.

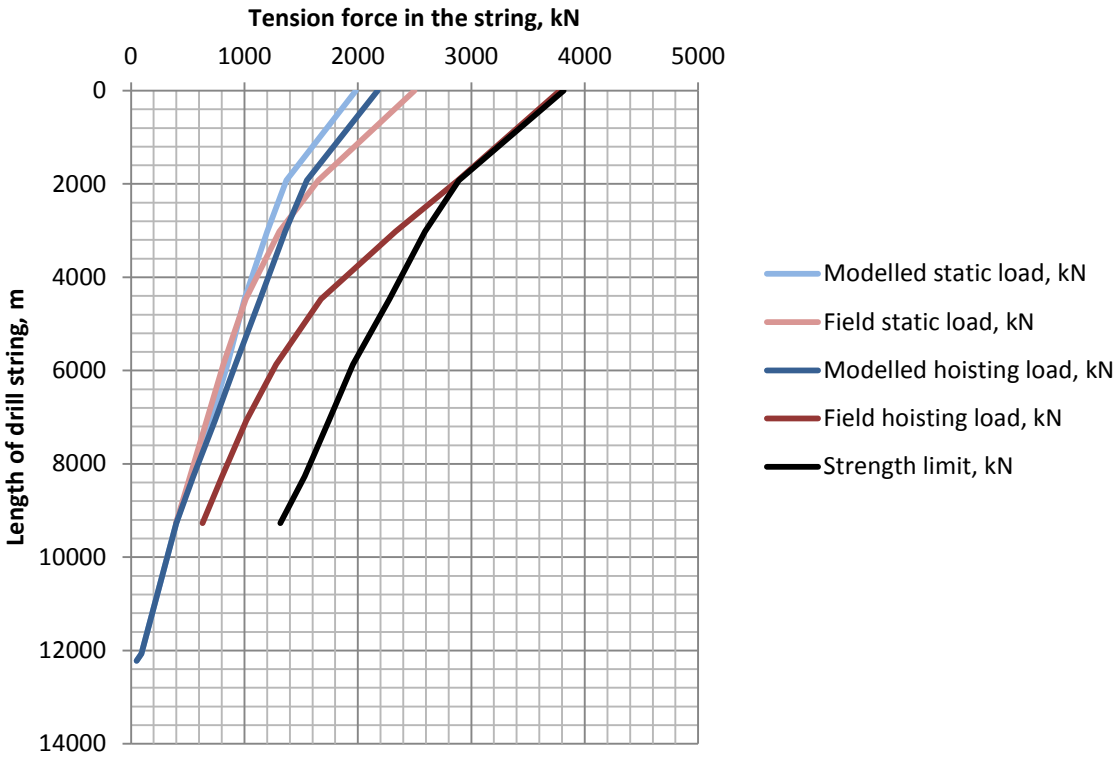

Fig. 20 Modelled and field loads along the length of drill-string.

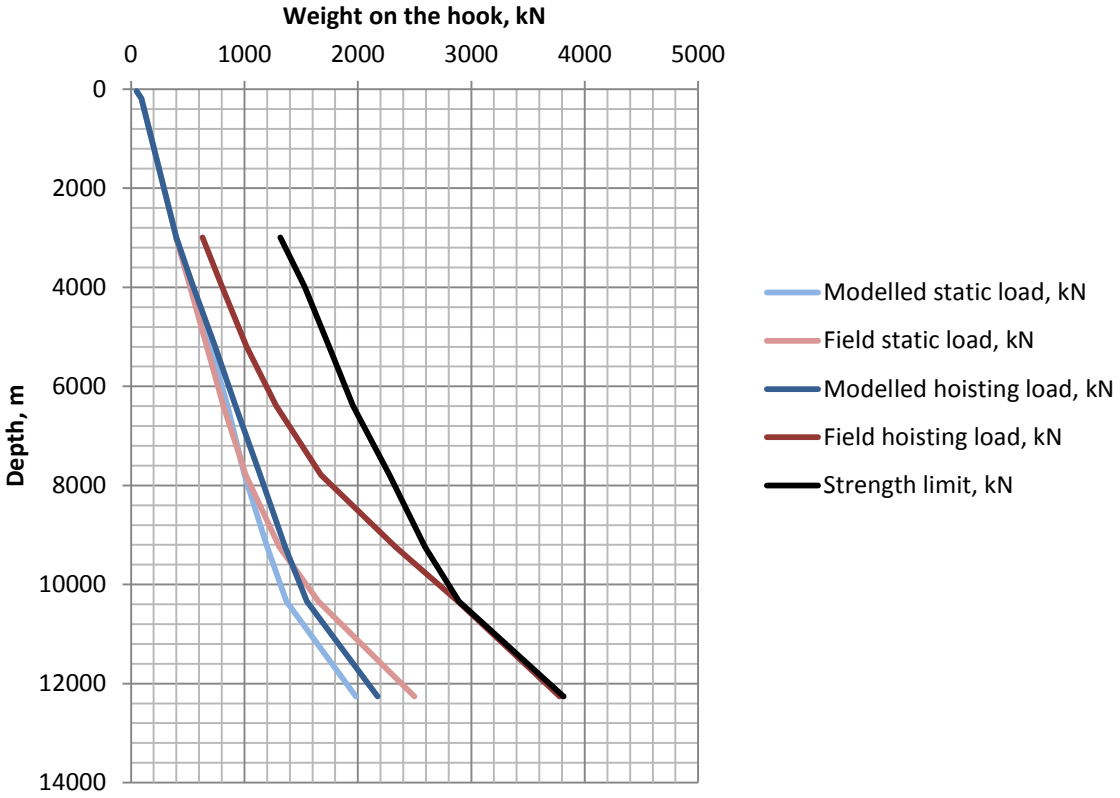

Fig. 21 Modelled and field loads on the hook against the drilled depth.

All this observations convince that well bore extensive collapse became the reason of insuperable difficulties of drilling. If under the drilling of first 7000 dominative problem was primary struggle with the curvature of well bore, then later the dominant issue becomes stability.

6 Modern approach of ultra-deep drilling

In the following chapter we will talk about the modern approach of drilling and look at all relative aspects concerning drill string evaluation. Will be proposed idea of double-wall drilling pipes and reviewed prospects of taking it into operation.

6.1 Eurasia project

Eurasia is a modern common international ultra-deep drilling project between Russia and Kazakhstan, which implementation started in 2015. Realization of the project intend to explore geological formation in the Caspian basin where concentrated about 80% of all hydrocarbon reserves of Kazakhstan. The planned depth of drilling reaches 15000 m. It is assumed to penetrate to this depth to get access for study of structure of sedimentary formations in the Caspian basin and possibly to find some hydrocarbons accumulations on the depth of 7-8 km. Place of well construction, which got the name of “Caspiy-1” assumed to be at the location of Chenkar Lake in Kazakhstan.

The average geothermal gradient at the location assumed to be around 26 ^{o}C per km. It is becomes an additional challenging problem to use high strength ADP. The allowable depth of descent here considering maximum operational temperature of aluminium resistive alloys AK1-T1 becomes around 10000 m. Properties of aluminium alloys presented in the table 7.

Among the possible solutions of ongoing project was proposed following ideas:

- Application of more durable and expensive steel types, yield strength of which exceeds 900 and 1000 MPa (P and T types in Russian mark definition; analogy of S-135 type with 930 MPa yield strength). Calculations showed that using S-135 steel the length of drill-string can be increased by 2000 m [11].
- Well known how the similar problem was decided using heavy sea water risers. On the riser strings was installed a few ejector floats which has increased buoyancy and reduced weight of the strings in the sea water.

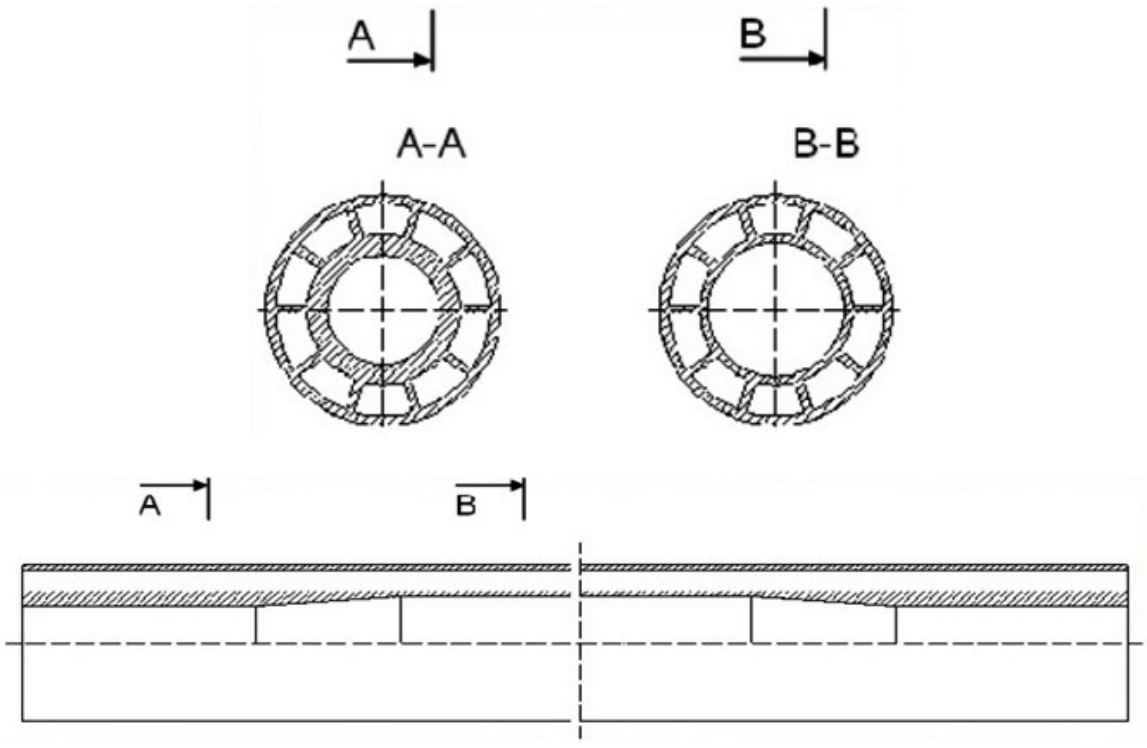

Fig. 22 Double-wall ADP proposed for drilling ultra-deep [11].

- There came an offer to use the pipes with double walls (fig. 22) proposed by I.Y. Balandin from Rosneft Scientific Research Center. It is also increases effect of buoyancy effect. Annular channel between the pipes walls filled with the air will be working as buoyancy floats for the drill-string [11].

To the disadvantages of the double wall aluminium drill-pipes (DWADP) can be attributed following:

- Reduced circulation mud passage between the pipe and bore-hole wall due to increased wall thickness. It is results in increase of hydraulic pressure component and bottom hole pressure for effective cleaning of the cuttings;
- Effect of internal and external pressure will be greater, then for the conventionally used pipe due to the higher difference in the pressure acting on each single wall;
- Increase of ribs number has a positive impact on the strength characteristics of the pipe but also leads to weight gain.

6.2 Evaluation of double-wall aluminium drill-pipes

For the analysis of the material used for drill-pipes manufacture can be used concept of maximal conditional drill-string length. This value indicates the maximum limited length of homogeneous drill-string suspended in the mud. At this length the pipe strength at the point of suspension reaches the limit of tensile load. Here temperature effect, frictional loads, safety factors and other parameters are not taken into account [11].

Max conditional drill-string length physically limited by the following expression:

$$F_{lim} \geq F_{DS\,mud} \tag{6.1}$$

Where F_{lim} - tension limit for the certain material, N; $F_{DS\,mud}$ - weight of drill-string in the mud, N.

Drill-string weight can be found from the following formula:

$$F_{DS\,mud} = L \cdot A \cdot \rho_{pipe} \cdot g \left(1 - \frac{\rho_{mud}}{\rho_{pipe}}\right) \tag{6.2}$$

Where L - length of the drill-string, m; A - cross-sectional area of pipe body, m^2; ρ_{mud} and ρ_{pipe} - density of mud solution and pipe material respectively, kg/m^3.

Max conditional drill-string length can be found by formula:

$$L_{max} = \frac{\sigma_y}{\rho_{pipe} \cdot g \left(1 - \frac{\rho_{mud}}{\rho_{pipe}}\right)} \tag{6.3}$$

For the drill-string combined of pipes having different cross-sectional area the formula taking following view:

$$L_{max} = \frac{F_{lim}}{\left(1 - \frac{\rho_{mud}}{\rho_{pipe}}\right)} \tag{6.4}$$

Where σ_y - yield strength of the pipe, N; f_{pipe} - average specific weight of the pipe in the air, N/m.

On the figures 23 illustrated calculated maximal conditional length of ordinary ADP having different alloys and different wall thickness. More data regarding computed maximal length for ADP and SDP of different alloys shown in the appendix.

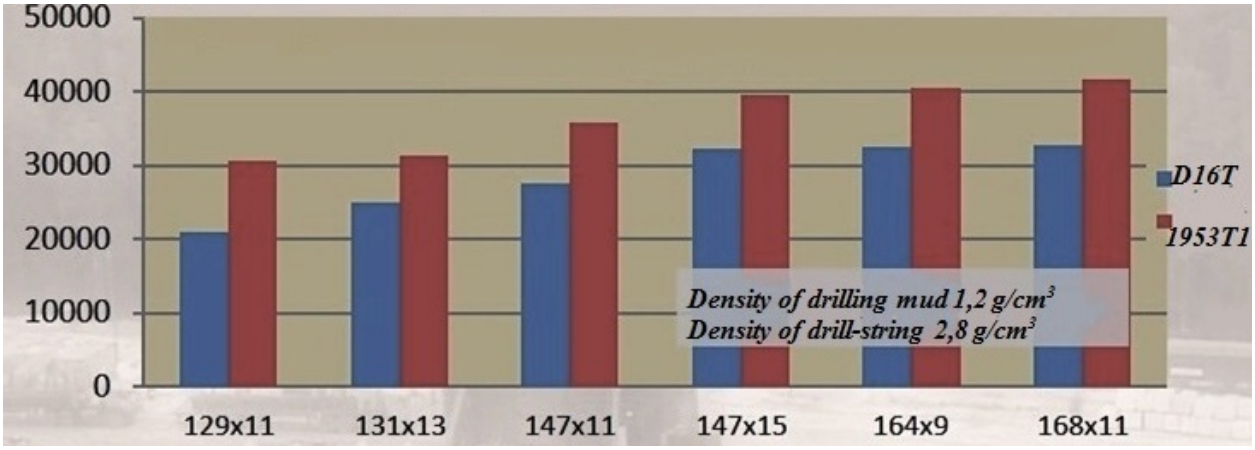

Fig. 23 Computed maximal conditional length of the drill-string combined of ADP from different type of alloys and having different wall thickness [11].

In case of double-wall pipes condition 6.1 modified in to following [11]:

$$F_{lim} \geq F_{DS\,air} - F_b \qquad (6.5)$$

Where $F_{DS\,air}$ – weight of drill-string in the air, N; F_b - buoyancy force, N.
Buoyancy force calculated by formula:

$$F_b = \rho_{mud} \cdot g \cdot L(A_{DS} + A_{air}) \qquad (6.6)$$

Where A_{DS} and A_{air} - cross-sectional area of metal and air channels respectively, m^2.

As a result we can get the formula for definition of maximal conditional length of double-wall drill-pipe. This equation is true for both double-wall steel drill-pipes (DWSDP) and DWADP [11]:

$$L_{max} = \frac{\sigma_y}{\rho_{pipe} \cdot g\left(1 - {\rho_{mud}}/{\rho_{pipe}} - {A_{air}\rho_{mud}}/{A_{DS}\rho_{pipe}}\right)} \qquad (6.7)$$

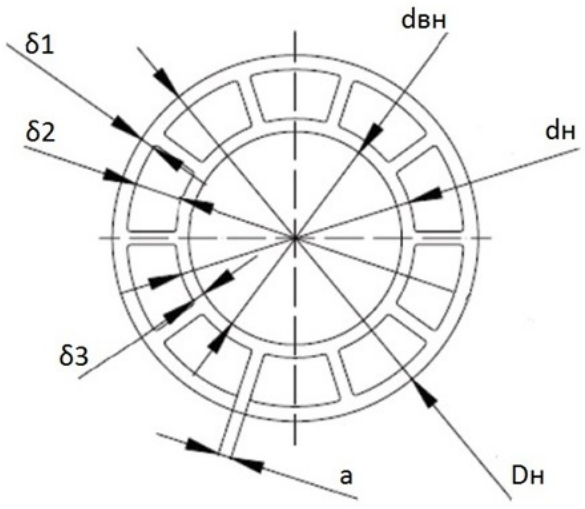

Fig. 24 Cross-section of DWADP[11].

On the figures 25 and 26 shown comparative charts of maximal conditional drill-string length for double-wall SDPs and ADPs respectively. As it seen from the bar charts, high density of the steel does not allow the buoyancy to make a positive effect on the length of drill-string. At the same time increase of air thickness between two walls of aluminium drill-pipe by 2 mm allow to elongate the maximal length by 5000-7000 m [11].

Figure 24 illustrating the cross-sectional specification of DWADP where walls has standard thicknesses of $\delta 1$ and $\delta 3$ equal to 9, 11, 13 and 15 mm.

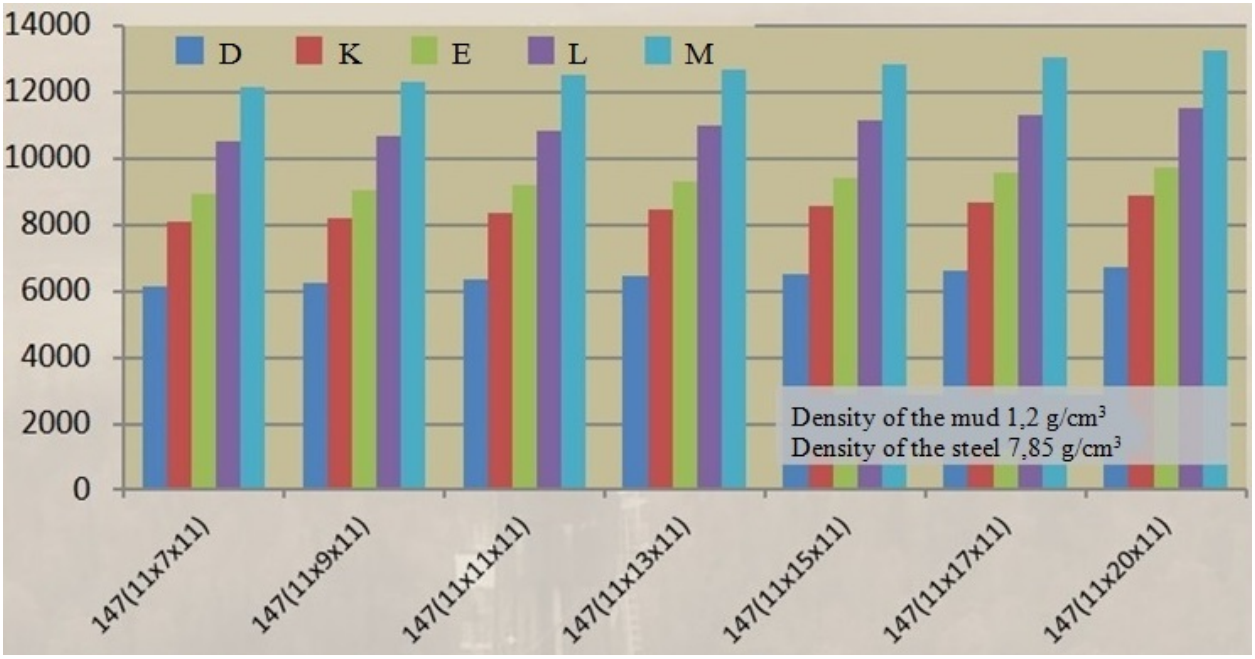

Fig. 25 Computed maximal conditional length of the drill-string combined of DWSDP from different type of alloys and having different wall thickness [11].

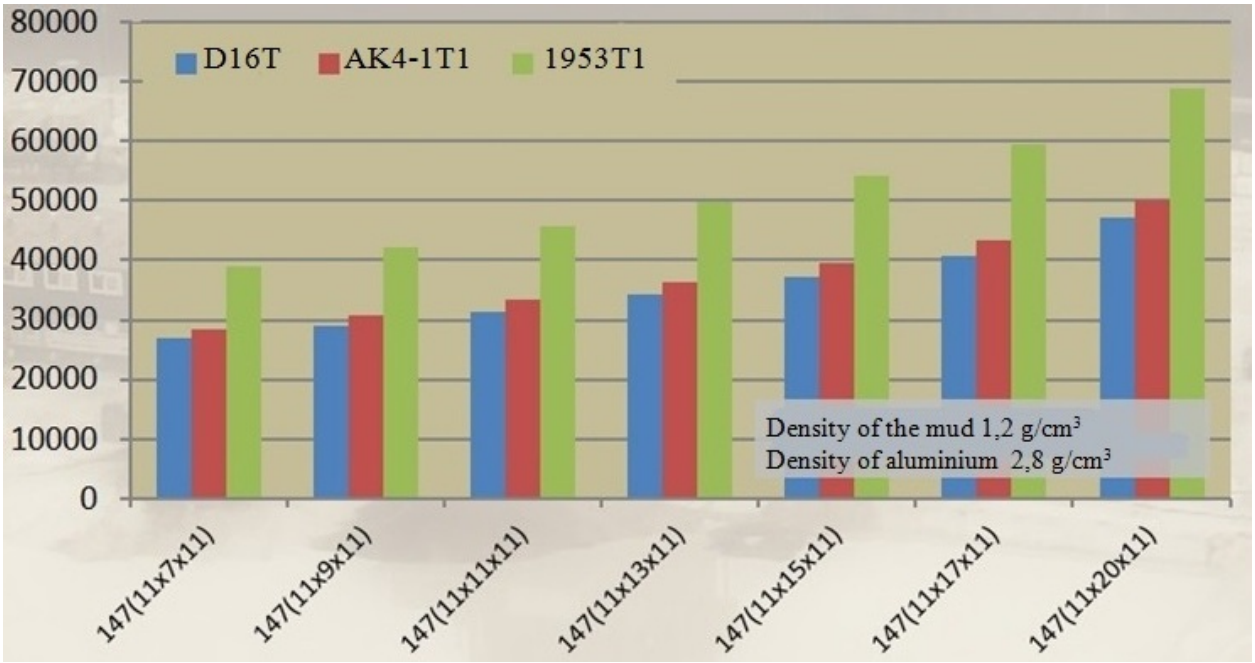

Fig. 26 Computed maximal conditional length of the drill-string combined of DWADP from different type of alloys and having different wall thickness [11].

Summarizing all mentioned above we can confidently assert that by inserting in the upper part of drill-string two or three sections of DWADP and using SDP or DWSDP sections in the high temperature zones it is possible to reach the planned depth of 15000 m. This challenge constitutes the future of engineering work of ultra-deep drilling.

7 Conclusion

Ultra-deep scientific drilling realized on Kola Peninsula provided the original chance to develop highly effective complex of technological tools and advanced drilling techniques, which were successfully transferred to the oil industry in a later years. Achieving of great drilling depth in very poor informational conditions was made possible by use of complex technical solutions such as:

- technique of pilot hole drilling;
- law rotational turbine method of drilling with use of reduction gear turbo-drills for hot wells (up to 250^{o}C);
- reliable high strength aluminium drill pipes;
- control devises for turbine with transmitting information to the surface;
- well-path control devices.

A number of techniques were successfully and widely field-tested:

- coring techniques for hard abrasive rocks;
- drilling and coring without pulling out drill-pipes using retractable drill bits and retrievable downhole motors;
- vertical drilling technology in hard unstable formations;
- procedures for borehole problems elimination in unstable formations;
- sidetracking techniques for super-deep intervals in hard formations.

Evaluation of Kola well and conducted calculations showed drag force nature and dependency of the well trajectory. We managed to show all aspects of drill-string evaluation for ultra-deep drill-string. Formation of all loads acting on the string and factors, which affects drill-string weakening and results in the pipe breakage.

Out of conducted evaluation we can make a conclusion that the principal difficulties were caused mainly by:

- high temperatures and pressures at great depths;
- increased weight of drill pipes and casings in the well;
- unpredicted wellbore stability problems;
- bending of the well-path;
- significant frictional forces in the well.

The drilling process may be improved by using heat-resistant rock-crushing tools and drilling fluids, by controlling pressures within the well, by struggle with the curvature and by increasing the strength and reliability of drill pipes. Analysis showed that requirements for allowable curvature of the well should be very strict because its lids to significant increase in the frictional forces and can be resulted in loss of kilometres of undrilled depth.

Without the past we cannot have a future and without noticeable outstanding project and its evaluation in the past we cannot come to the successful realization of the ultra-deep drilling in the future. Kola well became one of the strongest base on which experienced engineers could relay. Eurasia project described in the resent thesis became a logical continuation of developing idea of ultra deep scientific study. Evaluation and description of this particular study indicated high hidden potential in the use of double-wall aluminum drill-string.

Conducted and ongoing programs of ultra-deep scientific drilling have great benefit to the geological science in the understanding of earth crust features. Subject of ultra-deep drilling deserved high interest of international community and absolutely justified in the case of exploration study on the area having high economic potential.

References

[1] I. G. Apanovich and A. V. Orlov. (1970-1979). The Great Soviet Encyclopedia, 3rd Edition. *Ultra-deep drilling.* Retrived from http://encyclopedia2.thefreedictionary.com/Ultradeep+Drilling

[2] E. K. Semiletkova, A. P. Hupovka, I. P. Imochkina, L. F. Maklakova (1984). *Kola ultra-deep well.* Moscow: Publishing house: Nedra. Translated from Russian.

[3] B. S. Aadnøy (2010) *Modern Well Design*, 2d Edition, London. Publisher: Taylor & Francis Group.

[4] H. Rabia (1985) *Oilwell Drilling Engineering. Principles and Practice.* Publisher: Graham & Trotman

[5] B. S. Aadnøy, Reza Looyeh (2010) *Petroleum rock mechanics. Drilling operations and well design.* USA. Publisher: Elsevier.

[6] G. A. Krupennikov, P. A. Filatov (1972) *Stress distribution in rock formations.* Moscow: Publishing house “Nedra”. Translated from Russian.

[7] Y. A. Gelfgat, M. Y. Gelfgat, Y. S. Lopatin (2003) *Advanced drilling solutions. Lessons from FSU. Volume 2.* USA. Publisher: PennWell.

[8] B. S. Aadnøy, K. Larsen, P. C. Berg (1999) *Analysis of stuck pipe in deviated boreholes*. Journal of Petroleum Science and Engineering, USA. Publisher: Elsevier.

[9] B. S. Aadnoy, K. Andersen (2001) *Design of oil wells using analytical friction models.* Journal of Petroleum Science and Engineering, USA. Publisher: Elsevier.

[10] W. Scott, M. Mcdonough. Bright Hub Engineering (2010) *Metal alloys used in industry.* Retrieved from: http://www.brighthubengineering.com/manufacturing-technology/70222-metal-alloys-used-in-industry/ USA. Publisher: Bright Hub Inc.

[11] V.P. Balitsky, T. Y. Biktyakov, A. A. Statsenko (2015) *Design of drill-string for drilling ultra-deep wells.* Presentation.. Russian State Gubkin University of oil and gass. Russia.

List of abbreviations

BHA borehole assembly
TVD true vertical depth
TMD true measured depth
FSU formal Soviet Union countries
DWPP drilling and coring without pulling the drill-pipes
ADP aluminum drilling pipe
DWADP double wall aluminum drilling pipe
SDP steel drilling pipe
DWSDP double wall steel drilling pipe
OD outer diameter of the pipe
DL dog-leg
DLS dog-leg severity
RPM rotation per minute

List of figures and tables

Appendix

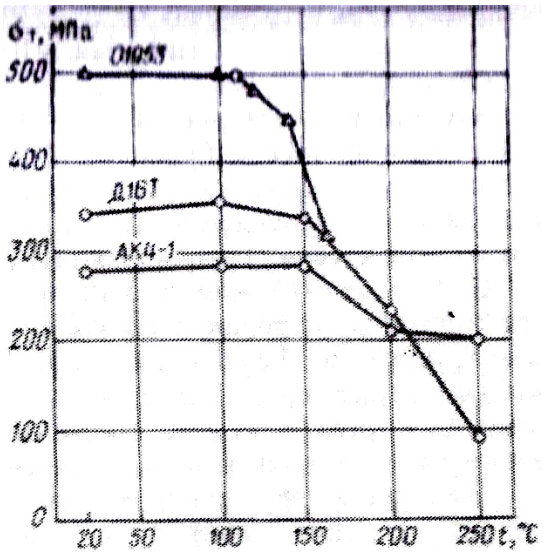

Fig. A Dependence between ADP alloys strength and the operational temperature.

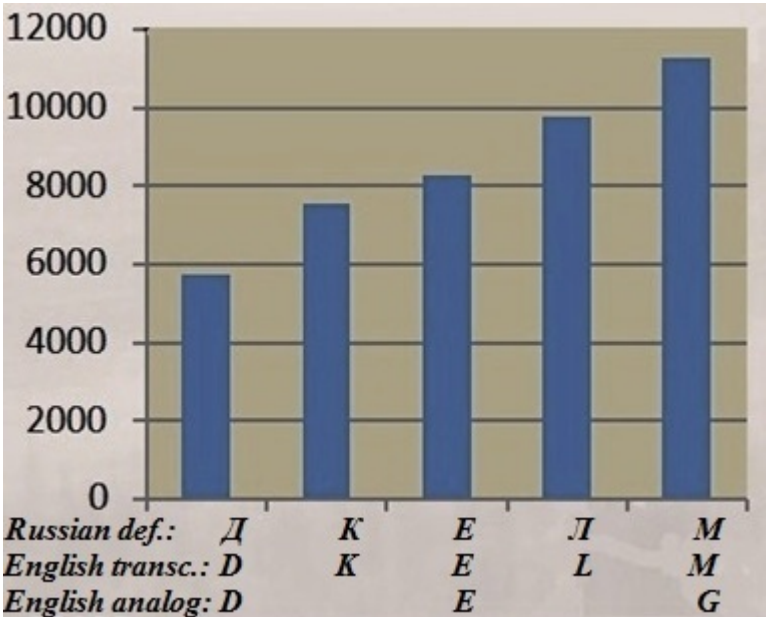

Fig. B Computed maximal conditional length of the drill-string combined of SDP from different type of alloys and having same wall thickness.

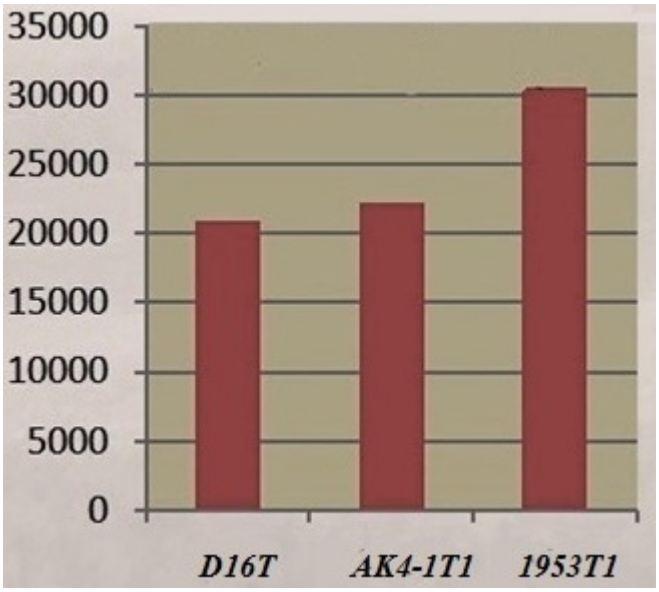

Fig. C Computed maximal conditional length of the drill-string combined of ADP from different type of alloys and having same wall thickness.

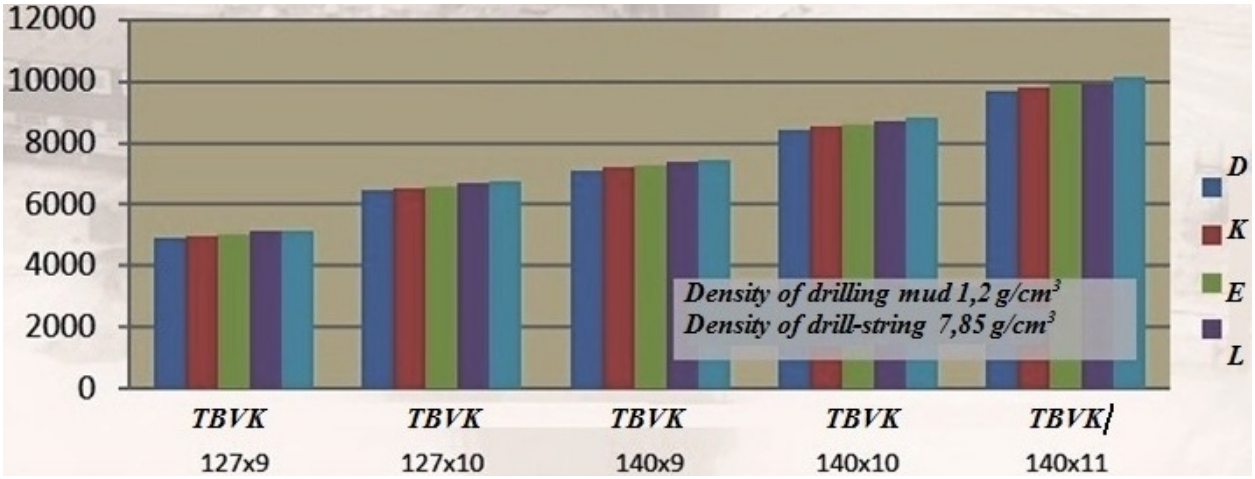

Fig. D Computed maximal conditional length of the drill-string combined of SDP from different type of alloys and having different wall thickness.